

1 **The impacts of mineral dust aerosols on global climate and**
2 **climate change**

3 Jasper F. Kok^{1,†}, Trude Storelvmo², Vlassis A. Karydis³, Adeyemi A. Adebiyi⁴, Natalie M. Mahowald⁵,
4 Amato T. Evan⁶, Cenlin He⁷ and Danny M. Leung¹

5 ¹Department of Atmospheric and Oceanic Sciences, University of California - Los Angeles, Los Angeles,
6 CA, USA

7 ²Department of Geoscience, University of Oslo, Oslo, Norway

8 ³Institute for Energy and Climate Research: Troposphere, Forschungszentrum Jülich GmbH, Jülich,
9 Germany

10 ⁴Department of Life and Environmental Sciences, University of California - Merced, Merced, USA

11 ⁵Department of Earth and Atmospheric Sciences, Cornell University, Ithaca, NY, USA

12 ⁶Scripps Institution of Oceanography, University of California, San Diego, CA, USA

13 ⁷Research Applications Laboratory, National Center for Atmospheric Research, Boulder, CO, USA

14 [†]email: jfkok@ucla.edu

17 **Abstract**

18 Mineral dust aerosols impact Earth's energy budget through interactions with radiation, clouds,
19 atmospheric chemistry, the cryosphere and biogeochemistry. In this review, we summarize these
20 interactions and assess the resulting impacts of dust, and of changes in dust, on global climate
21 and climate change. We find that the total effect of these interactions on Earth's global energy
22 budget—the dust effective radiative effect—is $-0.2 \pm 0.5 \text{ Wm}^{-2}$ (90% confidence interval).
23 Compared to pre-industrial times, global dust mass loading is $56 \pm 29\%$ higher in the modern
24 climate, leading to changes in the Earth's energy budget. Indeed, this increase in dust has
25 produced a global mean effective radiative forcing of $-0.07 \pm 0.18 \text{ Wm}^{-2}$. Current climate models
26 and climate assessments do not represent the historical increase in dust and thus omit the
27 resulting radiative forcing, biasing climate change projections and assessments of climate
28 sensitivity. Climate model simulations of future changes in dust diverge widely and are very
29 uncertain. Further work is thus needed to constrain the radiative effects of dust on climate and to
30 improve the representation of dust in climate models.

31

32 **Key points**

- 33 1. The direct radiative effect due to dust interactions with radiation is $-0.15 \pm 0.35 \text{ Wm}^{-2}$
34 and accounts for a large fraction of the dust effective radiative effect and its uncertainty.
- 35 2. Dust interactions with clouds, atmospheric chemistry, the cryosphere, and
36 biogeochemistry also contribute considerably to the uncertainty in the dust effective
37 radiative effect, in part because of a lack of observational constraints, which are urgently
38 needed.
- 39 3. Dust mass loading generated by all major source regions has increased since pre-
40 industrial times, namely by 47 (4-98) % for North African dust, by $76 \pm 39\%$ for Asian
41 dust, and by 27 (-17 to 95) % for Southern Hemisphere dust.
- 42 4. It is more likely that dust net cools than that it net warms global climate.
- 43 5. The historical increase in dust has likely somewhat counteracted greenhouse warming.

44 6. Careful simulations with coupled climate models that reproduce the historical dust
45 increase are needed to better constrain dust radiative forcing.
46
47

48 **Introduction**

49 Mineral dust aerosols are small rock-derived particles with diameter $D < \sim 100 \mu\text{m}$ that are
50 suspended in the atmosphere^{1,2}. Most dust is produced by the ballistic impacts of wind-driven
51 sand grains on sparsely vegetated and dry soils³, which ejects and fragments aggregates of soil
52 particles^{1,4}. Owing to these mechanical impacts, dust is a relatively coarse aerosol, with most of
53 its mass contained in the coarse ($D > 2.5 \mu\text{m}$) and super coarse ($D > 10 \mu\text{m}$) modes⁵.

54 Dust is produced in copious amounts in the world's deserts, loading the atmosphere with ~ 26
55 million tonnes of dust, which accounts for a large majority of the atmosphere's aerosol burden by
56 mass^{6,7}. The Sahara Desert and the Sahel contribute $\sim 50\%$ of global dust emissions (~ 2100
57 Tg/yr) and mass loading (~ 13 Tg), the Asian deserts $\sim 40\%$ (~ 2000 Tg/yr and ~ 10 Tg), and the
58 North American and Southern Hemisphere deserts and high latitude regions another $\sim 10\%$ (~ 500
59 Tg/yr and ~ 3 Tg) (Fig. 1)^{8,9}. Although much of the dust is deposited close to source regions, a
60 substantial fraction is transported for thousands of kilometres. For example, plumes of African
61 dust regularly travel across the tropical North Atlantic, reaching the southwestern United States
62 and the Amazon Basin¹⁰.

63 The abundance and long-range transport of dust cause it to impact climate through various
64 mechanisms. During transport, dust scatters and absorbs solar shortwave (SW) and terrestrial
65 longwave (LW) radiation^{6,11}, modifies cloud properties through seeding cloud droplets and ice
66 crystals^{12,13}, mixes with other aerosols¹⁴, and serves as a sink for radiatively important
67 atmospheric trace gases¹⁴⁻¹⁷. Upon deposition, dust darkens snow and ice packs^{18,19}, and
68 stimulates ecosystem productivity and CO₂ drawdown through the delivery of iron and
69 phosphorus²⁰. Because some of these mechanisms cool whereas others warm^{6,14,21}, it is unclear
70 whether dust exerts a net cooling or a net warming effect on global climate. Because
71 measurements of dust deposition suggest that dust has increased since the pre-industrial era^{22,23},
72 this uncertainty in the sign and magnitude of dust radiative effects means it is unknown whether
73 dust changes have enhanced or opposed anthropogenic warming.

74 In this review, we examine the impacts of dust, and of changes in dust, on global climate and
75 climate change. We first summarize the various mechanisms through which dust impacts Earth's
76 radiation budget, and assess the radiative effect produced by each mechanism. We then constrain
77 the increase in dust loading since pre-industrial times and assess the radiative perturbation
78 produced by this historical increase in dust. We also discuss the radiative perturbation due to
79 possible future changes in dust and end with recommendations for future research priorities.

80

81 **Mechanisms by which dust impacts climate**

82 Dust can perturb Earth's energy balance via various mechanisms. In each case, a radiative effect
83 arises, defined as the imbalance between incoming net solar radiation and outgoing infrared
84 radiation at the top-of-atmosphere (TOA) resulting from an atmospheric constituent (in this case,
85 dust)²⁴. These effects can be either instantaneous, such as scattering and absorbing SW and LW
86 radiation, or an adjustment, such as altering cloud cover²⁵.

87 We calculate the radiative effect due to mechanism i in the modern climate, r_i (Wm⁻²), as the
88 change in Earth's energy balance, Δf_i (Wm⁻²), produced per change in global dust mass loading
89 from modern levels, ΔL_i (Tg), multiplied by the global modern dust loading, L (Tg). That is,

$$r_i \equiv \frac{\Delta f_i}{\Delta L_i} L. \quad (1)$$

90 The sum of all radiative effects then equals the effective radiative effect of dust, R (Wm⁻²),
 91 which includes both instantaneous radiative effects and adjustments^{25,27},

$$R = \sum_i r_i. \quad (2)$$

92 Eqs. (1) and (2) define the dust effective radiative effect in such a way that it can be used to
 93 obtain the radiative perturbation, ΔF , due to a change in dust loading, ΔL_m , from its value in the
 94 modern climate,

$$\Delta F = R \frac{\Delta L_m}{L}. \quad (3)$$

95 We then define the effective radiative forcing of dust due to the change $\Delta L_{p \rightarrow m}$ in dust mass
 96 loading from pre-industrial to modern times as

$$\Delta F_{p \rightarrow m} = R \frac{\Delta L_{p \rightarrow m}}{L}. \quad (4)$$

97 Our use here of the term radiative forcing deviates slightly from previous work^{25,27} in which it
 98 denotes radiative perturbations that are entirely from anthropogenic forcing agents. However,
 99 because dust is a natural aerosol affected by climate changes and human land use changes, a
 100 radiative perturbation due to a historical change in dust can be partially due to both human land
 101 use changes (a forcing) and natural and anthropogenic climate changes (a feedback). Because
 102 these two contributions are difficult to disentangle, we refer to the entire radiative perturbation
 103 due to the historical change in dust as the **dust** effective radiative forcing.

104 Radiative effects from dust arise through interactions with radiation, atmospheric chemistry,
 105 clouds, the cryosphere, and biogeochemistry (**Fig. 2**). Each of these mechanisms are now
 106 discussed.

107 *Interactions with radiation*

108 Perhaps the best understood mechanism by which dust impacts climate is through the dust direct
 109 radiative effect (DRE), the perturbation of Earth's energy balance by scattering and absorption of
 110 radiation (**Fig. 2a**). Since dust spans a wide range of sizes, from ~0.1 – 100 μm²⁹, it interacts
 111 with both SW (centered around 550 nm wavelength) and LW (centered around 10 μm
 112 wavelength) radiation^{30,31}.

113 The sign and magnitude of the dust DRE depend on the balance between these interactions. For
 114 instance, scattering of SW radiation cools the climate while absorption of SW radiation warms,
 115 with an overall net cooling^{6,32}. In contrast, scattering and absorption of LW radiation both warm
 116 the climate since both decrease the transparency of the atmosphere to terrestrial LW radiation³³.
 117 Thus, the balance between cooling from SW scattering, and warming from SW absorption and
 118 LW scattering and absorption, dictate the dust DRE.

119 For SW radiation, the balance between scattering and absorption is influenced by dust particle
 120 size. Because absorption increases more strongly with particle size than scattering^{34,35}, the single-
 121 scattering albedo (SSA; the ratio of scattered radiation to total extinguished radiation) decreases
 122 with particle size. Indeed, submicron dust has an SSA close to 1, whereas supermicron dust
 123 absorbs a substantial fraction of extinguished radiation, exhibiting SSAs of ~0.95 at $D = 2$ μm,
 124 ~0.80 at $D = 10$ μm, and even lower for super coarse dust^{30,36}.

125 However, the exact SSA of dust aerosols depends on their complex refractive index, determined
126 by particle mineralogy³¹. Absorption increases approximately linearly with iron oxide content,
127 which is primarily provided by hematite and goethite³⁷. Dust optical properties can also be
128 affected by mixing with other aerosols, especially black carbon³⁸. Observations suggest that this
129 possible mixing has limited impact on the optical properties of most African dust^{39,40}, but could
130 substantially affect those of East Asian dust⁴¹.

131 Although dust particle size and mineralogy determine the balance between SW scattering and
132 absorption, the efficiency with which both processes perturb the TOA radiative flux depends on
133 the albedo of the underlying surface. Indeed, the cooling effect of SW scattering is enhanced if
134 the dust is situated above dark (low albedo) surfaces like the ocean and forests that would
135 otherwise absorb most of the radiation⁴². Conversely, the warming effect of SW absorption is
136 enhanced if the dust is situated above clouds or above high albedo land surfaces like snow, ice,
137 and deserts that would otherwise scatter most of the radiation back to space^{35,43}.

138 Dust microphysical properties and mineralogy also influence the extinction of LW radiation. For
139 example, because of its longer wavelengths, LW radiation is extinguished primarily by coarse
140 dust^{30,33,44}. The sensitivity of LW extinction to mineralogy is less important than for SW
141 interactions owing to the smaller variability in LW optical properties between minerals, and
142 because LW scattering and absorption both warm the planet^{31,45,46}.

143 The efficiency with which dust extinction of LW radiation perturbs the TOA radiative flux also
144 depends on the atmosphere's transparency to LW radiation and the elevation of the dust layer.
145 Indeed, the TOA flux is only substantially impacted if the atmosphere is at least somewhat
146 transparent to LW radiation, as is the case in the absence of clouds in the ~8 – 13 μm
147 'atmospheric window' wavelength range^{33,47}. Furthermore, because LW emission depends on
148 temperature, the LW warming depends on the temperature difference between the dust layer and
149 the source of the LW radiation - usually the surface or clouds below the dust layer. In addition,
150 the atmosphere's transparency to LW radiation decreases with the concentration of water vapor
151 and thus increases with height. As such, dust warming by LW extinction increases approximately
152 linearly with the height of the dust layer^{33,42,47,48}.

153

154 Although the processes by which dust interacts with SW and LW radiation are relatively well
155 understood, the resulting radiative effects are poorly constrained. For dust interactions with SW
156 radiation, central estimates of SW DRE are -0.40 Wm^{-2} (-0.10 to -0.70 Wm^{-2} , 90% confidence
157 interval)^{6,32,49-53} (**Fig. 3**); these estimates are determined using less absorbing optical properties
158 and a coarser dust size distribution, consistent with experimental constraints^{4,6,29,37,40,54-56}. The
159 wide range reflects substantial uncertainties in the dust size distribution⁶ and dust optical
160 properties⁴⁶. For dust interactions with LW radiation, best estimates of LW DRE are $+0.25 \text{ Wm}^{-2}$
161 with a range of $+0.10$ to $+0.40 \text{ Wm}^{-2}$ (**Fig. 3**)^{6,32,46,49-52}; these estimates use realistic optical
162 properties⁴⁵ and size distributions that are consistent with satellite constraints on the LW direct
163 radiative effect^{48,57}. The range reflects uncertainties in dust LW optical properties⁴⁵, the height of
164 dust plumes^{58,59}, the dust size distribution and the contribution of super coarse dust^{36,49,54}, and the
165 effect of LW scattering by dust, which is neglected in climate models^{32,33} and is sometimes
166 accounted for using a simple correction factor^{6,32,46,52}.

167 As a result of the uncertainties and opposing SW and LW DRE, it is unclear whether the dust
168 DRE exerts a net cooling or warming effect. Combining the SW and LW DRE yields a net dust

169 DRE of $-0.15 \pm 0.35 \text{ Wm}^{-2}$, consistent with other calculations^{6,32,46,49-51} (**Fig. 3**). As such, the
170 dust DRE could either slightly warm or substantially cool the planet, or it could have little net
171 impact. We assign medium confidence to this assessment because of the large body of research
172 and availability of satellite-based constraints.

173 ***Interactions with atmospheric chemistry***

174 Dust affects atmospheric chemistry through numerous interactions with atmospheric trace gases
175 and aerosols. Although freshly emitted mineral dust is considered insoluble, it is reactive towards
176 trace acidic gases derived from anthropogenic pollutants and sea salt^{17,60}. Mineral dust particles
177 collected throughout the world are notably associated with nitrate⁶¹⁻⁶³. Nitric acid interacts with
178 the non-volatile mineral cations of dust, forming salts to maintain the charge balance in the
179 aerosol phase⁶⁴. The uptake of such acidic vapors is very rapid due to their ability to react with
180 carbonates and other minerals through simple acid-base chemistry⁶⁵. Over continents, such
181 interactions of mineral cations with anthropogenic sulfuric acid causes the accumulation of
182 substantial amounts of sulfate on dust surfaces⁶⁶. In contrast, over oceans, mineral cations are
183 commonly associated with chloride derived from sea salt⁶⁷.

184 Mineral dust also provides surfaces for the adsorption of inorganic (notably SO_2 , NO_2 , and O_3)
185 and organic trace gases¹⁷, affecting the optical properties, hygroscopicity and atmospheric
186 residence time of both dust and anthropogenic aerosols. Therefore, dust particles provide a
187 substantial sink for the direct removal of important atmospheric constituents like O_3 , affecting
188 the oxidative capacity of the atmosphere and the ozone radiative forcing^{68,69}. Dust particles also
189 provide reaction sites for the oxidation of SO_2 to sulfuric acid⁷⁰ and the formation of nitrous acid
190 through heterogeneous reactions of NO_2 ⁷¹. However, such heterogeneous formation of salts
191 occurs at a much slower pace than through the direct uptake of acidic vapours since acid
192 anhydrides (for example SO_2) do not initially contain any acidic protons⁶⁵. Additionally, the high
193 pH values found on the alkaline mineral particles can promote the formation of ammonium
194 nitrate on their surface^{72,73}.

195 All these interactions of dust with atmospheric gases can transform the surface and even the bulk
196 chemical composition of dust particles^{74,75}. This chemical processing of dust is highly dependent
197 on both the gas phase composition and on the dust chemical composition^{64,76}, which depends on
198 the mineralogy of the source soil⁷⁷.

199 The chemical ageing of dust due to these various reactions creates a soluble coating that
200 increases the dust particle's hydrophilicity, which in turn affects the residence time of dust and
201 its interactions with clouds. For example, the interaction of a calcite-containing dust particle with
202 nitric acid converts the insoluble calcium carbonate to the highly hygroscopic calcium nitrate⁷⁸.
203 The increased hygroscopicity of the chemically aged dust increases its water adsorption
204 efficiency, making it grow more rapidly under humid conditions, thus causing it to form cloud
205 droplets and extinguish radiation more efficiently. On the contrary, the increased water uptake by
206 the large, aged dust particles can also deplete in-cloud supersaturation, thereby reducing the
207 number of smaller anthropogenic particles that are activated and grow into cloud droplets¹³.
208 Furthermore, chemical ageing of mineral dust can also reduce its ice nucleating ability⁸⁰.

209 These heterogeneous and multiphase reactions affect the atmospheric loading of both dust and
210 non-dust aerosols. Nitrate formation associated with the mineral cations removes nitric acid from
211 the gas phase, decreasing the formation of ammonium nitrate aerosols. Similarly, sulfate
212 formation on dust decreases SO_2 abundance and thus the formation of sulfate aerosols. As such,

213 dust can reduce the concentration of anthropogenic CCN both by adsorption of precursor gases
214 and through coagulation with anthropogenic aerosols. Furthermore, the hygroscopic growth of
215 aged dust can increase its scavenging and deposition rate, reducing its atmospheric residence
216 time and loading^{15,81}. However, modelling results suggest that these effects can enhance the total
217 accumulation mode dust burden through a reduced loss by coagulation with coarse dust
218 particles¹⁵.

219 The physicochemical interactions of mineral dust with atmospheric composition can thus affect
220 the direct and indirect radiative forcing of both dust and non-dust aerosols (Fig. 2b). These
221 effects can be both negative or positive, depending on the region and the prevailing impacts of
222 dust on the atmospheric aerosol loading and composition^{15,16}. A net cooling effect of -0.05 Wm^{-2}
223 has been calculated for the effect of dust on the total aerosol DRE¹⁵, driven mostly by an
224 enhanced burden of the accumulation mode dust aerosols and decreased absorption of SW
225 radiation due to the modified aerosol composition of mineral dust. However, observations of dust
226 during transport across the Atlantic and Mediterranean oceans indicate that the size distribution
227 of dust with diameters less than $5 \mu\text{m}$ remains remarkably constant and that optical properties do
228 not change appreciably^{39,40,55}. Moreover, a critical effect of heterogeneous chemistry on dust
229 surfaces is to reduce the atmospheric loading of anthropogenic aerosols, thereby decreasing their
230 direct radiative cooling, resulting in a net warming of $+0.12$ to $+0.20 \text{ Wm}^{-2}$ ^{16,82,83}. Overall, the
231 impact of dust interactions with atmospheric chemistry on the aerosol DRE is highly uncertain.
232 The resulting radiative effect is assessed at $0.10 \pm 0.15 \text{ Wm}^{-2}$ to encompass the possibility of the
233 slight cooling of -0.05 Wm^{-2} ¹⁵ as a lower bound and the larger warming found by others^{16,82,83} as
234 an upper bound. We assign very low confidence to this assessment.

235 *Interactions with clouds*

236 Dust particles influence clouds via multiple interactions, including changing the thermodynamic
237 environment by absorbing SW and LW radiation and serving as cloud condensation nuclei
238 (CCN) and ice-nucleating particles (INPs). Radiative perturbations produced by dust effects on
239 warm clouds, mixed-phase clouds, cirrus (ice) clouds, and by semi-direct effects are discussed
240 next.

241 *Dust indirect effects on warm clouds*

242 There are three main pathways through which dust particles can affect warm clouds: first,
243 by increasing the concentration of CCN, as laboratory studies have shown that various types of
244 (unprocessed) mineral dusts possess a modest ability to act as CCN^{84,85}, which is further
245 enhanced by atmospheric processing (ageing) of dust⁸⁶; second, by reducing the concentration
246 of non-dust CCN through coagulation and adsorption of precursor gasses; and third by acting as
247 giant CCN, which can form cloud droplets at relatively low supersaturation and thus deplete
248 water vapor to such an extent that overall cloud droplet formation is suppressed. The second and
249 third pathways are both thought to reduce cloud droplet number concentrations (CDNC), and
250 thus reduce cloud albedo and shorten cloud lifetimes.

251 Although some modelling results found that the pathways that decrease CDNC dominate (Fig.
252 2c, lower branch), amounting to a decrease of as much as -11% in the global mean CDNC¹³,
253 most other modelling has found that dust slightly increases the global mean CDNC abundance.
254 These latter results thus suggest that the effect of dust acting as CCN dominates (Fig. 2c, upper
255 branch), albeit with large differences in the magnitude of the dust-induced CDNC

256 contribution^{21,87,88}. As a CDNC increase is expected to increase cloud albedo and extend cloud
257 lifetime through well-established mechanisms²⁸, a dust-induced increase in CDNC would have a
258 net cooling effect (Fig. 2c, upper branch). For example, global simulations with the CAM5
259 model²¹ resulted in a ~1% increase in CDNC for a 3-fold increase in dust emissions, and this
260 CDNC increase in turn produced a negative forcing of -0.01 Wm⁻². Such an effect is indeed
261 supported by estimates based on satellite observations⁸⁹.

262 Although past work thus reached contradictory conclusions regarding the net global effects of
263 dust on warm clouds, there is broad agreement that the sign and magnitude of the dust
264 contribution to CDNC is highly heterogeneous in both space and time^{13,21}. Given the relatively
265 sparse research and disagreement on the sign of the global mean CDNC contribution from dust,
266 we assess the corresponding perturbation to Earth's TOA radiation budget through changes to
267 liquid clouds to likely be negative but close to zero, with an uncertainty range of -0.10 to +0.10
268 Wm⁻². This assessment is based on scaling the estimates of CCN/CDNC changes^{13,21,87,88} with
269 the forcing estimate per change in CCN/CDNC cited above²¹, and has low confidence.

270 *Dust indirect effects on mixed-phase clouds*

271 Although the ability of dust to act as CCN is somewhat ambiguous, their ice-nucleating ability is
272 undisputed^{90,91}. A wide variety of dust particles have been investigated in the laboratory and
273 found to be efficient INPs both in the immersion mode (freezing cloud droplets from within) and
274 in the deposition mode (nucleating ice through vapor depositing onto them, possibly triggered by
275 freezing of condensed water in particle pores⁹²). The former is the ice formation mechanism
276 thought to be of greatest relevance for mixed-phase clouds (MPCs). These are clouds with
277 temperatures between approximately -38°C and 0°C that can consist of either supercooled liquid
278 droplets, ice crystals, or a mixture. MPCs are generally optically thick and efficiently reflect
279 incoming SW radiation (a cooling effect). Their optical thickness also allows them to absorb
280 virtually all outgoing LW radiation, reducing the amount of LW radiation emitted to space (a
281 warming effect). The former (SW) effect has been found to dominate in the global mean⁹³. In an
282 INP-limited ("pristine") environment, MPCs will be optically thick and usually have liquid cloud
283 tops⁹⁴, with only small amounts of ice residing in the cloud interior or below cloud base as ice
284 crystals rapidly grow and sediment out (Fig. 2d, left schematic). In a dust-enriched environment,
285 MPCs will be partly or completely glaciated, depending on the dust abundance and INP
286 efficiency. This cloud glaciation results in an overall reduction of cloud albedo and thus a
287 positive (warming) radiative effect (Fig. 2d, right schematic). An increase in dust loading, and
288 thus INPs, therefore likely produce a warming effect on climate by reducing the cooling effect of
289 MPCs (Fig. 2d).

290 Modelling results on the effects of dust on MPCs generally agree qualitatively, but differ
291 quantitatively. Global simulations with the E3SM model⁹⁵ found that dust effects on mixed-
292 phase clouds perturb the TOA radiation budget by +0.05 to +0.26 Wm⁻². This perturbation arises
293 from a reduction in cloud liquid water and a corresponding increase in cloud ice (Fig. 2d). For
294 comparison, global simulations with the CAM5 model estimated that going from a very pristine
295 state with only 10% of current dust emissions to present-day dust emissions induced a
296 perturbation of only 0.01 to 0.10 Wm⁻² through dust-INP effects on mixed-phase clouds, again
297 by shifting cloud phase in favor of more ice²¹. However, as the atmospheric dust loading change
298 in the latter study is smaller than in the former, these estimates are broadly consistent with each
299 other. These modelling results are further supported by satellite observations that found that dust-
300 enriched environments tend to have MPCs with a larger proportion of ice than their counterparts

301 in largely dust-free environments^{96,97}. Thus, a perturbation to the TOA radiation budget of
302 approximately 0.10 Wm^{-2} due to dust effects on MPCs is supported, but with a relatively large
303 assessed uncertainty range of 0 to 0.20 Wm^{-2} and low confidence, owing to the limited body of
304 research.

305 *Dust indirect effects on cirrus clouds*

306 The dominant role of dust particles in cirrus cloud formation worldwide is supported by in situ
307 measurements, satellite observations, and numerical modelling^{98,99}. Cirrus clouds are pure ice
308 clouds residing in the upper troposphere at temperatures below approximately -38°C . These
309 clouds have a net warming effect on climate by reducing emission of LW radiation to space more
310 effectively than they reflect SW radiation¹⁰⁰. Cirrus clouds can form by two different
311 mechanisms: homogeneous freezing, in which small solution droplets freeze spontaneously, and
312 heterogeneous freezing, in which ice crystals form on INPs⁹¹. The latter mechanism requires
313 only modest supersaturation but can only occur when sufficient INPs are present and typically
314 results in low concentrations of large ice crystals. The former mechanism requires much higher
315 supersaturation but does not rely on the presence of INPs and typically results in high
316 concentrations of small ice crystals¹². The transition from homogeneous to heterogeneous
317 freezing has been estimated to occur for INP concentrations between 10 and 100 L^{-1} .¹⁰¹

318 The impact of dust on cirrus clouds is thus highly dependent on whether non-dust INPs are
319 present (Fig. 2e). In conditions that favor heterogeneous freezing (high INP concentration),
320 additional dust INPs would add ice crystals and reduce their size, while in conditions that favor
321 homogeneous freezing (low INP concentration), additional dust could reduce the number of ice
322 crystals and increase their size by shifting nucleation from occurring homogeneously to
323 occurring heterogeneously. The former scenario would make cirrus clouds optically thicker and
324 extend their lifetimes, while the latter scenario would do the opposite.

325 The perturbation of the TOA radiation budget would naturally be opposite in the two scenarios,
326 and at present it is unclear which one dominates globally. Thus, although global modelling
327 results of dust impacts on cirrus clouds have in the past produced net radiative perturbations of
328 opposite sign¹², this difference does not signify a complete lack of process understanding, but
329 rather indicates different assessments of which cirrus formation mechanism dominates in the
330 absence of dust.

331 Research that incorporated up-to-date laboratory results of ice nucleation on dust
332 particles^{92,102,103} generally find an optical thinning of cirrus clouds due to dust (Fig. 2e, top
333 schematic). This thinning yields large opposing perturbations to both LW and SW radiation at
334 the TOA, but the LW effect tends to dominate, producing a net negative (cooling)
335 perturbation^{21,104}. The corresponding overall radiative effect was estimated at -0.4 Wm^{-2} using
336 global simulations with the CAM5 model¹⁰⁴, whereas simulations for a more moderate dust
337 change (going from 10% to 100% of present emissions) with a modified version of the same
338 model²¹ found a range from -0.32 to $+0.05 \text{ Wm}^{-2}$. We therefore assess the perturbation of the
339 TOA radiation budget due to dust effects on cirrus clouds to -0.20 Wm^{-2} , with a 90% confidence
340 interval of -0.40 to $+0.10 \text{ Wm}^{-2}$. This range encompasses the strongest reported cooling effects¹⁰⁴
341 as a lower bound and the possibility of a slight warming as an upper bound. We assign low
342 confidence to this assessment due to the limited body of research.

343 *Dust semi-direct effects on clouds*

344 Absorption of radiation by mineral dust can modify the temperature profile¹⁰⁵, which can change
345 atmospheric stability, the moisture profile, and secondary circulations, all of which can alter
346 cloud distributions¹⁰⁶⁻¹⁰⁸. These processes, known as aerosol semi-direct effects (SDEs)^{109,110},
347 were broadly described in the IPCC's Sixth Assessment Report as atmospheric adjustments to
348 instantaneous aerosol direct radiative effects without considering effects due to changes in
349 surface temperature^{25,28}. Because dust accounts for about a third of shortwave absorption by all
350 aerosols, the contribution of dust to SDEe is crucial to accurately quantifying the overall dust
351 effective radiative forcing^{111,112}.

352 The magnitude of the dust SDE, and whether it results in a positive (warming) or a negative
353 (cooling) radiative effect, depends primarily on two factors: the relative position of the dust and
354 cloud layers within the atmospheric column and the amount of radiation absorbed by the dust
355 layer^{106,107}. In turn, radiation absorption by dust depends on dust loading and microphysical
356 properties, including dust mineralogical composition, shape, and size distribution^{42,43,45,113}.

357 Understanding of the pathways through which dust semi-directly impacts different cloud regimes
358 follows that of SDEs produced by other absorbing aerosols, like black carbon^{106,114}. For low-
359 altitude clouds, the pathways for dust SDEs can be categorized into cases where the dust layer is
360 above, within or near, and below the cloud layer (Fig. 2f). When dust is located above boundary-
361 layer clouds, local heating by the above-cloud dust can stabilize the boundary layer by
362 strengthening its capping inversion, causing an increased build-up of moisture in the boundary
363 layer. This increased moisture increases the cloud cover, which results in a negative SDE (left
364 schematic of Fig. 2f)^{107,115}. Conversely, when dust is located within or near boundary-layer
365 clouds, the local heating could result in reduction of relative humidity, which could evaporate the
366 cloud and result in a positive SDE (middle schematic of Fig. 2f)^{107,116}. Finally, when dust is
367 located below boundary-layer clouds, the local heating may enhance convergence and available
368 moisture, increasing cloud cover and resulting in a negative SDE (right schematic of Fig.
369 2f)^{117,118}.

370 Radiation absorption by dust can also generate SDEs for mid and high-altitude clouds. These
371 SDEs involve the compensation between the warming effect produced by dust absorption, which
372 tends to decrease cloud cover, and an increase in moisture convergence, which tends to increase
373 cloud cover¹⁰⁶. Although the effect of the enhanced moisture convergence can overwhelm the
374 warming effect, resulting in increased globally averaged high-altitude cloud cover during the
375 summer, the overall annual-mean dust SDE is to decrease the high cloud cover^{106,119,120}.

376 This understanding of dust SDEs assumes that dust, like other absorbing aerosols such as black
377 carbon, warms the atmospheric layer in which they are present¹²¹. This assumption is based on
378 evidence that dust radiative warming due to SW absorption dominates over dust radiative
379 cooling due to LW emission^{122,123}. However, past research likely underestimated the amount of
380 coarse dust, which emits LW radiation more strongly than fine dust^{49,56}. Because accounting for
381 the observed abundance coarse dust particles could produce substantial LW radiative cooling of
382 the atmosphere^{32,36,124}, the understanding of the different pathways through which dust can semi-
383 directly impact clouds remains incomplete.

384 Because of the uncertainties in the various pathways by which dust absorption semi-directly
385 influences cloud cover (Fig. 2f), a global observational estimate of dust SDE is not currently
386 available. Instead, observationally based assessments have focused on dust-dominated
387 regions^{107,116,125}. For example, satellite observations show that annual dust SDE is negative (-1.2

388 $\pm 1.4 \text{ Wm}^{-2}$) over the North Atlantic Ocean¹⁰⁷. Since estimates of dust SDE show strong spatial
389 variability and because dust SDE is driven by different dominant mechanisms for different cloud
390 regimes over the ocean than over land¹⁰⁶, scaling such observationally based regional dust SDE
391 estimates to global values is difficult. In addition, accurate retrievals of dust microphysical
392 properties, including dust optical properties and size distribution, are lacking from global-scale
393 satellite and ground-based platforms¹¹², making it difficult to obtain global estimates of dust
394 SDE.

395 In the absence of global observational estimates, climate models simulations have reported a net
396 positive global annual mean dust SDE¹²⁶. These estimates vary by over an order of magnitude,
397 between 0.01 and 0.16 Wm^{-2} , and depend on the climate model used^{21,126,127}. These positive SDE
398 estimates are consistent with an overall decrease in cloud cover in these simulations. Although
399 model estimates of dust SDE and cloud changes are thus relatively consistent with each other,
400 they could be biased because of unaccounted for uncertainties in dust absorption properties, the
401 vertical distributions of dust and clouds, an underestimate of LW radiative cooling by coarse
402 dust, and the parameterization of cloud processes^{56,58,111}. Therefore, based on the above model
403 simulations, the dust SDE is estimated at $0.07 \pm 0.07 \text{ Wm}^{-2}$, but with low confidence due to these
404 possible biases and limited research.

405 *Interactions with the cryosphere*

406 Dust interactions with the cryosphere impact climate by altering cryospheric conditions via dust
407 direct and indirect radiative effects (Figs. 2a-f) and by darkening snow and ice surfaces after
408 deposition (Fig. 2g), which leads to a positive surface radiative effect (Fig. 2g). This dust-
409 induced snow albedo effect accelerates snow and glacier melting^{18,128,129}, which triggers a strong,
410 positive surface albedo feedback on the climate system¹³⁰. The dust-induced snow albedo effect
411 is influenced by many factors, including dust concentration in snow^{131,132}, dust optical properties
412 as determined by its size distribution and chemical composition^{132,133}, dust-snow mixing
413 state^{134,135}, snow grain size and shape¹³⁴, snowpack properties^{136,137}, and illumination
414 conditions^{132,138}.

415 Observations indicate strong heterogeneity in dust concentrations in snow/ice. Along with
416 different snowpack and atmospheric conditions, this variability in dust concentrations leads to
417 large variations in the dust-induced snow albedo reduction and the associated surface radiative
418 effects. For instance, the springtime dust-induced snow albedo effect is estimated to be less than
419 0.5 Wm^{-2} for the Arctic^{139,140}, up to 5 Wm^{-2} for remote mid-latitude snowpacks (such as the
420 Tibetan Plateau)^{139,141}, and about $10\text{--}50 \text{ Wm}^{-2}$ over polluted mid-latitude snowpacks (such as the
421 U. S. Rocky Mountains)^{18,128}. In some extremely polluted mid-latitude mountains, the local
422 instantaneous snow albedo effect can be as high as $100\text{--}300 \text{ Wm}^{-2}$ ^{142,143}. The dust-induced snow
423 albedo effect is typically larger in aged snow than in fresh snow¹⁸, because of the stronger light
424 penetration and hence larger light absorption by dust in aged snow. Most research has focused on
425 a few cryospheric hotspots in the Northern Hemisphere (the Rocky Mountains, Tibetan Plateau,
426 European Alps, and the Arctic) during spring, when the dust-induced snow albedo effect is more
427 prominent and often reaches its annual maximum.

428 There are only limited estimates of the global annual mean dust-induced snow albedo effect,
429 with a central estimate of $+0.013 \text{ Wm}^{-2}$ and a 90% confidence interval of $0.007\text{--}0.03 \text{ Wm}^{-2}$
430^{19,131,144}. Although the snow albedo radiative effect is smaller than most other dust radiative

431 effects, it can still be more substantial regionally, particularly over polluted mid-latitude
432 snowpacks¹⁸.

433 Estimates of the dust-induced snow albedo effect are still associated with large uncertainties due
434 to complicated and poorly constrained dust-snowpack-radiation interactions. Variations in the
435 poorly constrained dust-snow mixing state, snow grain shape, dust size distribution and dust
436 chemical composition can cause up to a factor of two uncertainty in the dust-induced snow
437 albedo effect^{134,135}. Moreover, the limited knowledge of dust evolution within the snowpack - for
438 instance due to dust scavenging by melting water and dust enrichment at the snowpack surface -
439 also adds to the uncertainty of the estimated snow albedo effect. Owing to the potential
440 nonlinearity in dust-snow-radiation interactions and dust wet deposition, the dust-induced snow
441 albedo effect may not increase linearly with dust concentration in the atmosphere or snowpack.
442 Considering these uncertainties and the limited research, we assign low confidence to our
443 estimate of the dust-induced snow albedo effect.

444 *Interactions with biogeochemistry*

445 Dust can influence ocean and land biogeochemistry, both directly through the addition of
446 nutrients and pollutants to ecosystems, as well as indirectly through modifying precipitation,
447 temperature, and radiation²⁰. Atmospheric deposition of dust onto oceans provides iron, a
448 limiting nutrient in high nutrient low chlorophyll (HNLC) regions^{145,146}. In addition, nitrogen
449 fixing organisms in the ocean have higher iron requirements, thereby linking iron deposition to
450 the oceanic nitrogen cycle^{147,148}. Although initial research suggested that atmospheric deposition
451 was the dominant source of new iron^{145,149}, other ocean sources also have a substantial role in the
452 iron cycle¹⁵⁰⁻¹⁵². Overall, atmospheric inputs of iron to the ocean modulate ecosystem
453 productivity and carbon sequestration on the timescale of decades^{146,153}.

454 , The soluble fraction of the iron is the most important for dust particles sinking through the
455 ocean mixed layer. The deposition of soluble iron has increased since pre-industrial times, both
456 because of the historical increase of dust over this time period and because of an increase in iron
457 solubilization during transport due to increased anthropogenic pollution^{22,154,155}. Additionally,
458 some other important sources of soluble iron have also increased, including from wildfires and
459 anthropogenic combustion^{156,157}. The resulting alleviation of iron limitation has increased
460 ecosystem productivity, which in turn has reduced the atmospheric concentration of carbon
461 dioxide and its radiative forcing (Fig. 2h).

462 Several ocean biogeochemical models include iron and its coupling to the nitrogen cycle and can
463 therefore estimate the reduction of CO₂ concentrations due to the alleviation of iron
464 limitation^{158,159}. These models suggest that the increased deposition of soluble iron over the 20th
465 century resulted in the uptake of ~4 ppm of CO₂, producing a radiative perturbation of -0.07 ±
466 0.07 Wm⁻²^{20,160}. Because approximately half of this increase in soluble iron was estimated to be
467 due to a simulated ~40% increase in dust over the 20th century, these results imply a radiative
468 effect due to dust-biogeochemistry interactions of -0.12 ± 0.12 Wm⁻² (Eq. 1). Confidence in this
469 assessment is very low, as it is based on only one study. Note that the radiative effect due to
470 dust-biogeochemistry interactions differ from that due to other interactions in that its effect
471 increases over time. Consequently, the radiative perturbation that it produces depends on the
472 timescale.

473 Dust also contains phosphorus, a limiting nutrient in some tropical forests and grasslands^{161,162},
474 as well as in some ocean ecosystems^{146,163}. For example, phosphorus from long-range transported

475 North African dust may help maintain the productivity of the Amazon rainforest¹⁶⁴. However,
476 because inputs from atmospheric deposition of desert dust are thought to be important in the
477 Amazon on millennial time scales¹⁶⁵ any contribution of changes in this phosphorus input
478 probably produces a negligible contribution to dust radiative forcing since pre-industrial times.
479 Dust also serves as a ballast, enhancing the downward transfer of organic material within the
480 ocean, but there is not yet a quantitative estimate of the impacts in terms of productivity or
481 carbon uptake feedback from this process^{170,171}. In addition, desert dust could include elements
482 that can be toxic to ocean or land ecosystems, such as Cu, although current estimates suggest that
483 this effect is not important to Earth's radiation budget¹⁷².

484 **The dust effective radiative effect**

485 To determine the climatic impact of past and future changes in atmospheric dust, it is critical to
486 assess the dust effective radiative effect R (Eq. 2), which equals the sum of the various radiative
487 effects generated by dust (Fig. 3). Many of these radiative effects oppose one another, resulting
488 in a median estimate of $R = -0.2 \text{ Wm}^{-2}$, with a wide 90% confidence interval of -0.7 to +0.3 Wm^{-2} .
489 (Note that we neglected some rapid adjustments in assessing R , such as responses by water
490 vapor and the lapse rate to dust direct radiative effects, but these adjustments are likely small¹⁷³.)
491 As such, the net effect of dust on Earth's global radiation budget could be negligible, a
492 substantial net cooling, or a small net warming.

493 On regional scales and for different seasons, the dust effective radiative effect can differ
494 substantially from its global and annual mean in Figure 3. This regional and seasonal variability
495 occurs because the various radiative effects are sensitive to the spatiotemporal variability in dust
496 concentration, microphysical properties (mineralogy and size distribution), and environmental
497 conditions (surface albedo and cloud cover). For instance, dust over reflective deserts likely
498 produces substantial warming because of the high dust concentration, coarse size distribution¹²⁴,
499 and because reflective surfaces reduce cooling produced by SW scattering and enhance warming
500 produced by SW absorption^{35,174}. Similarly, dust likely produces net warming over snow and ice-
501 covered regions because the high surface albedo enhances warming produced by dust absorption
502 of SW radiation and because dust deposition decreases the surface albedo^{42,131}. In contrast, dust
503 over oceans usually produces cooling because dust is finer further from source regions and
504 because the ocean albedo is only ~0.1 in the visible spectrum¹⁷⁵. To determine the climate
505 impacts of dust, it is thus critical not only to constrain the global mean dust effective radiative
506 effect but also to constrain its spatiotemporal pattern.

507 **Dust radiative forcing**

509 Because dust produces a potentially large effective radiative effect, a change in atmospheric dust
510 loading since pre-industrial times could have produced a substantial effective radiative forcing.
511 Dust loading could have changed due to both climate change and widespread human land use
512 changes (Box 1). Knowledge of the change in dust loading from pre-industrial to modern times
513 depends largely on dust deposition records that resolve both the modern and the pre-industrial
514 climate. Many of these deposition records show increases in dust deposition between modern and
515 pre-industrial times, sometimes by a factor of ~4^{23,169,176,177}.

517 We reconstructed the evolution of the global dust mass loading since pre-industrial times by
518 combining 22 dust deposition records^{23,169,176,177} with constraints on the source regions providing
519 the deposition flux to each deposition core^{8,44} (see Supplementary Information). This dust
520 reconstruction used a bootstrap resampling method to propagate uncertainties in both the
521 experimental deposition records and the constraints on source region-resolved deposition fluxes
522 to each deposition site; nonetheless, errors should be interpreted as a lower bound.

523 The atmospheric loading of dust with a volume-equivalent diameter less than 20 μm has
524 increased from 19 ± 6 Tg in the pre-industrial period (defined here as 1841-1860) to 30 ± 8 Tg in
525 the modern climate (1981-2000). As such, global dust mass loading has increased by 56 ± 29 %
526 (Fig. 4a). Although substantial, this increase is less than the doubling of dust suggested by
527 previous research^{22,23}. A large contributor to this increase has been Asian dust, which has
528 increased by 76 ± 39 % from 8 ± 3 Tg in pre-industrial times to 14 ± 5 Tg in modern times (Fig.
529 4c). North African dust has increased less, from 9 (6-14) Tg in the pre-industrial period to 14 ± 4
530 Tg in the modern climate, representing a 47 (4-98) % increase. Both African and Asian dust
531 mass loading peaked in the 1980s and then decreased substantially, consistent with changes
532 observed from long-term dust concentration measurements, visibility records, and satellite
533 observations¹⁷⁸⁻¹⁸⁴. Dust has likely also increased in the Southern Hemisphere, from 1.2 (0.6-2.2)
534 Tg to 1.5 (0.8-2.4) Tg, representing a 27 (-17 to 95) % increase (Fig. 4d). Satellite observations
535 suggest that global dust mass loading has been relatively stable since the year 2000, the end point
536 of the analysis, with some notable regional trends, such as in Central and East Asia¹⁸⁵.

537 This large historical increase in dust mass loading is inadequately accounted for in current
538 climate models and climate assessments. In fact, twelve climate models with prognostic dust
539 cycles in the Coupled Model Intercomparison Project phase 6 (CMIP6) model ensemble^{186,187}
540 show little change in dust mass loading since pre-industrial times (Fig. 5). This failure of models
541 to reproduce the historical dust increase could be due to several reasons (Box 1). If the dust
542 increase has been largely driven by natural and anthropogenic climate changes, then the model
543 failure could be either due to an inaccurate representation of these changes in models or because
544 modelled dust emissions are not sufficiently sensitive to changes in climate. This latter
545 possibility is suggested by the common use in climate models of empirical dust source functions
546 to parameterize the spatial distribution of dust emissions^{188,189}. Because dust source functions are
547 static, they mask physical links between changeable surface properties and dust emissions. As
548 such, their use can cause models to underestimate the sensitivity of dust emissions to changes in
549 climate¹⁹⁰. Conversely, if the dust increase has been largely driven by human land use changes
550 (Box 1), as suggested by research indicating that approximately a quarter of current dust
551 emissions originate from regions heavily impacted by human land use¹⁹¹ (Box 1), then the model
552 failure to reproduce the dust increase could be caused by an underestimation of land use and land
553 cover changes in drylands and the resulting increases in dust emissions.

554 *Radiative forcing due to dust increase*

555 The historical increase in dust loading could have produced a substantial radiative forcing.
556 Combining $R = -0.2 \pm 0.5 \text{ W m}^{-2}$ with the $56 \pm 29\%$ historical dust loading increase yields a dust
557 effective radiative forcing from 1841 to 2000 of $\Delta F_{\text{p} \rightarrow \text{m}} = -0.07 \pm 0.18 \text{ W m}^{-2}$. Dust radiative
558 forcing could thus either have substantially contributed to, or slightly opposed, the total aerosol
559 effective radiative forcing of -1.1 (-1.7 to -0.4) W m^{-2} for the period of 1750 to 2019²⁸.

560 Note that the calculations of R and $\Delta F_{p \rightarrow m}$ are subject to important limitations. First, these
561 calculations assume that radiative effects increase linearly with aerosol loading^{6,192} (Eqs. 3 and
562 4). However, the increase of radiative effects with aerosol loading is usually less-than-linear,
563 especially for interactions with clouds and biogeochemistry^{20,21,26}. Moreover, the radiative effects
564 of dust vary in space, such that $\Delta F_{p \rightarrow m}$ depends on the spatial pattern of dust increases, which the
565 simple calculation here does not account for. For instance, Asian dust likely has an outsize
566 impact on Northern Hemisphere cirrus clouds⁹⁸ and high latitude dust emissions are likely
567 important in controlling the glaciation of mixed-phase clouds^{193,194} but are not explicitly included
568 in the dust reconstruction. Careful simulations with coupled climate models that reproduce the
569 historical dust increase are thus needed to better constrain dust radiative forcing.

570 Because current climate models do not reproduce the historical dust increase, these models omit
571 the potentially important radiative forcing due to increased dust interactions with radiation,
572 clouds, atmospheric chemistry and the cryosphere. (Note that changes in CO₂ and other
573 greenhouse gases due to dust interactions with biogeochemistry are inherently included in
574 climate model runs forced by observed greenhouse gas concentrations.) Dust radiative forcing
575 was thus not accounted for in constraints on the total aerosol effective radiative forcing in the
576 IPCC Sixth Assessment Report²⁸. Because constraints on climate sensitivity depend strongly on
577 the aerosol radiative forcing since pre-industrial times¹⁹⁵, the failure by models and climate
578 assessments to account for the historical increase in dust could thus have biased constraints on
579 climate sensitivity and projections of future climate changes¹⁹⁶.

580

581 **Future changes in dust radiative forcing**

582 Future changes in dust radiative forcing are likely to be dominated by changes in atmospheric
583 dust loading, which in turn will be determined by several factors. One important factor will be
584 future changes in soil moisture since drier soils are more susceptible to aeolian erosion because
585 of reduced soil cohesive forces and less vegetation^{1,2}. In CMIP5 and CMIP6 models, changes in
586 precipitation are the main driver of soil moisture changes, yet there is a wide degree of
587 divergence in model projections of precipitation¹⁹⁷. Models do consistently show that as the
588 planet warms the evaporative demand over land increases¹⁹⁸, which by itself would reduce soil
589 moisture. However, the effects of reduced soil moisture may be countered by CO₂ fertilization,
590 which reduces plant water losses. This could reduce dust emissions by driving an expansion of
591 vegetation into arid regions¹⁹⁹, although the magnitude of this effect is uncertain²⁰⁰. Terrestrial
592 stilling, the observed downward trend in surface wind speeds over land surfaces²⁰¹, could also
593 affect dust emissions, with models suggesting a future reduction in Northern Hemisphere winds
594²⁰². However, changes in atmospheric circulation patterns thought to impact surface wind speeds
595 over dust producing regions may be more important¹⁸⁰. Another consequence of planetary
596 warming is an increase in precipitation variability²⁰³, and thus extreme rainfall events²⁰⁴,
597 potentially increasing future sediment supply—and aeolian erosion—via alluvial and fluvial
598 recharge²⁰⁵. Finally, future climate and land use changes could drive a decline in biological soil
599 crusts that reduce dust emissions, which is a mechanism for increasing emissions that is not
600 accounted for in current models²⁰⁶.

601 Model estimates of future changes in dust are sensitive to methodology²⁰⁷ and span the range of
602 an increase in dust due to increasing aridity²⁰⁸ to a decrease due to CO₂ fertilization driving an
603 expansion of vegetation into arid regions^{199,209}. Starting with CMIP5, simulations from some

604 models included either prescribed dust emissions or fully interactive dust. However, both
605 regional^{189,210-212} and global²¹³ analyses of these models found that the dust mean state had
606 substantial biases, that CMIP5 models did not reproduce historical dust variability, and that
607 modelled dust emissions were insufficiently sensitive to changes in surface conditions. An
608 analysis of dust changes over land in RCP 8.5 simulations, for which CO₂ emissions continue
609 unabated throughout the 21st century, showed no secular trends in global dust²¹³. An analysis of
610 CMIP6 simulations demonstrated that many of these previously identified model deficiencies
611 also exist in these newer climate model simulations (Fig. 5) and that the inter-model differences
612 in dust are also growing relative to earlier CMIP efforts, suggesting that as model complexity
613 increases so does model divergence in future projections of dust²¹⁴.

614 Given the inability of models to reproduce historical dust changes and the large spread in model
615 projections of future dust change, it is not surprising that estimates of the change in dust radiative
616 forcing per degree planetary warming, the so-called dust-climate feedback (units Wm⁻²K⁻¹), is
617 similarly uncertain. An analysis of the output from 6 CMIP6 models that participated in an
618 aerosol intercomparison project found that these models differed in the sign of the dust-climate
619 feedback¹⁸⁷, with a multimodel mean feedback of $0.0026 \pm 0.0048 \text{ Wm}^{-2}\text{K}^{-1}$. Other research has
620 speculated that a key driver of the model inconsistencies was the simulation of surface winds¹⁸⁷,
621 which in turn may be related to the relatively coarse resolution of a typical climate model²¹⁵.
622 These results from CMIP6 are consistent with earlier research that estimated a multimodel mean
623 feedback for CMIP5 models that was not statistically different from zero²¹⁶. However, using a
624 dust emission scheme that responded more realistically to changes in climate²¹⁷ enhanced the
625 dust climate feedback due to changes in the dust direct radiative effect by an order of magnitude,
626 yielding a range of -0.04 to +0.02 Wm⁻²K⁻¹. On a regional scale, the dust climate feedback close
627 to source regions is likely an additional order of magnitude larger²¹⁶.

628 Given the lack of confidence in model projections of future changes in the dust burden, and the
629 substantial uncertainties in dust direct and indirect radiative effects, there is a low degree of
630 confidence in the ability of models to predict future changes in the dust radiative forcing.

631 **Summary & Future Perspectives**

632 We assessed the global mean effective radiative effect of dust in the modern climate at $R = -0.2$
633 $\pm 0.5 \text{ Wm}^{-2}$ (Fig. 3). Despite the considerable uncertainty in the sign and magnitude of R , which
634 arises from the numerous uncertain and sometimes opposing mechanisms through which dust
635 impacts climate, it is more likely that dust cools than that it warms global climate. We further
636 found that global dust loading in the modern climate is $56 \pm 29\%$ higher than it was in pre-
637 industrial times (Fig. 4), which has exerted a global mean effective radiative forcing of $\Delta F_{p \rightarrow m} =$
638 $-0.07 \pm 0.18 \text{ Wm}^{-2}$. The historical increase in dust has thus likely somewhat counteracted
639 greenhouse warming.

640 Current climate models fail to capture the historical increase in dust loading (Fig. 5) and thus
641 inadequately account for dust radiative forcing, which could have caused biases in assessments
642 of climate sensitivity and projections of future climate changes^{195,196}. Substantial additional
643 research is thus needed both to better constrain R and $\Delta F_{p \rightarrow m}$ and to enable climate models to
644 reproduce the historical increase in dust.

645

646 The dust direct radiative effect (DRE) contributes most to the uncertainty in R and $\Delta F_{p \rightarrow m}$ (Fig.
647 3). Future research should focus on reducing its uncertainty by better constraining dust optical
648 properties through *in situ* and remote sensing observations. For instance, the information on soil
649 mineralogy to be provided by NASA's 2022 Earth Surface Mineral Dust Source Investigation
650 (EMIT) mission could help constrain dust optical properties²¹⁸. Additionally, models likely
651 greatly underestimate the atmospheric concentration of super coarse dust^{49,55,56,124}, which warms
652 by absorbing SW and LW radiation. This should be addressed by obtaining more measurements
653 of emitted and transported dust that extend to the difficult-to-measure super coarse dust size
654 range^{29,36,54,55}, and by developing improved parameterizations of super coarse dust emission²²⁰
655 and deposition and implementing those in climate models.

656 Another priority for future research should be better constraining the radiative effects of dust due
657 to interactions with clouds, anthropogenic aerosols, and biogeochemistry, which together
658 contribute the remaining uncertainty in R (Fig. 3). Because of a dearth of observational
659 constraints, our assessment of these radiative effects was mostly based on modelling studies.
660 However, models struggle to correctly account for interactions of dust with clouds and
661 anthropogenic aerosols, in part because of the mismatch in scales between the small scales at
662 which the relevant processes occur and the large scales of climate model grid boxes^{38,219,221}. As
663 such, there is an urgent need for comprehensive *in situ* and satellite observations to constrain
664 these interactions^{12,193}. For instance, more satellite and *in situ* observations of cirrus interactions
665 with dust and other INPs^{98,99} could elucidate the relative importance of homogeneous and
666 heterogeneous nucleation of ice crystals, which determines the sign of the radiative effect of dust
667 interactions with cirrus (Fig. 2e)¹². Furthermore, dust radiative effects due to interactions with
668 clouds could be better constrained with future model simulations at a sufficiently high
669 (kilometre-scale²²¹) resolution to resolve the critical sub-grid scale turbulence and cloud
670 processes that currently must be parameterized in models²¹⁹. Finally, constraining radiative
671 effects due to dust interactions with biogeochemistry requires an improved characterization of
672 dust composition and how this evolves during transport, as well as accurate knowledge of which
673 land and ocean regions are nutrient limited¹⁵³.

674 We also recommend that the community conducts multi-model experiments to obtain more
675 robust estimates of the various dust radiative effects and of R and $\Delta F_{p \rightarrow m}$. These experiments
676 should also investigate the uncertainty in radiative effects that result from model differences in
677 dust optical properties, size distribution, model resolution, meteorology, the spatiotemporal
678 distribution of dust emission fluxes, and parameterizations for dust deposition and dust
679 interactions with clouds, radiation, atmospheric chemistry, the cryosphere, biogeochemistry, and
680 other aerosols. Such multi-model experiments could be done in the context of the Aerosol Model
681 Intercomparison project (AeroCom), which has previously performed multi-model experiments
682 for anthropogenic aerosols^{25,222}.

683 Future research should also prioritize addressing the failure of models to reproduce the historical
684 increase in dust (Fig. 5). Doing so requires an improved understanding of the factors driving
685 changes in the atmospheric dust loading since pre-industrial times, including the relative roles of
686 changes in land use, wind speed, soil properties, sediment supply, and vegetation cover^{180,223}.
687 Additionally, new observations and modelling are needed to clarify the meteorological processes
688 that generate the high wind speeds that produce dust, such as cold pool outflows from moist
689 convection^{215,224,225}, and to improve the representation of those processes in climate models.
690 Finally, more physically based dust emission schemes need to be developed and implemented

691 into climate models. These schemes should explicitly account for dust emissions from high
692 latitudes, which have an outsize effect on climate through interactions with clouds^{193,194}.
693 Furthermore, dust emission schemes should avoid using empirical dust source functions as these
694 do not respond to changes in climate; instead, emission schemes should use process
695 understanding to account for the dependence of the spatiotemporal pattern and mineralogical
696 composition of dust emissions on wind, soil properties, sediment supply, and vegetation
697 coverage^{190,226,227}. A challenge will be to achieve this without making these schemes too
698 sensitive to parameters such as soil moisture that non-linearly increase dust emissions^{1,2} and that
699 have considerable variability in climate models¹⁹⁷. These fundamental improvements in dust
700 emission schemes are also needed for meaningful predictions of future changes in dust and for
701 more accurate predictions of dust impacts on regional climate.

702

703 References

- 704 1 Shao, Y. P. *Physics and Modelling of Wind Erosion*. 2nd edn, (Springer, 2008).
- 705 2 Kok, J. F., Parteli, E. J. R., Michaels, T. I. & Karam, D. B. The physics of wind-blown
706 sand and dust. *Rep. Prog. Phys.* **75**, 106901, doi:10.1088/0034-4885/75/10/106901
707 (2012).
- 708 3 Gillette, D. A. On the production of soil wind erosion having the potential for long range
709 transport. *J. Rech. Atmos.* **8**, 734-744 (1974).
- 710 4 Kok, J. F. A scaling theory for the size distribution of emitted dust aerosols suggests
711 climate models underestimate the size of the global dust cycle. *Proc. Natl. Acad. Sci. U.*
712 *S. A.* **108**, 1016-1021, doi:10.1073/pnas.1014798108 (2011).
- 713 5 Mahowald, N. *et al.* The size distribution of desert dust aerosols and its impact on the
714 Earth system. *Aeolian Res.* **15**, 53-71, doi:10.1016/j.aeolia.2013.09.002 (2014).
- 715 6 Kok, J. F. *et al.* Smaller desert dust cooling effect estimated from analysis of dust size
716 and abundance. *Nature Geoscience* **10**, 274-278, doi:10.1038/ngeo2912 (2017).
- 717 7 Gliss, J. *et al.* AeroCom phase III multi-model evaluation of the aerosol life cycle and
718 optical properties using ground- and space-based remote sensing as well as surface in situ
719 observations. *Atmospheric Chemistry and Physics* **21**, 87-128, doi:10.5194/acp-21-87-
720 2021 (2021).
- 721 8 Kok, J. F. *et al.* Contribution of the world's main dust source regions to the global cycle
722 of desert dust. *Atmospheric Chemistry and Physics* **21**, 8169-8193, doi:10.5194/acp-21-
723 8169-2021 (2021).
- 724 9 Bullard, J. E. *et al.* High-latitude dust in the Earth system. *Reviews of Geophysics* **54**,
725 447-485, doi:10.1002/2016rg000518 (2016).
- 726 10 Prospero, J. M., Delany, A. C. & Carlson, T. N. The Discovery of African Dust Transport
727 to the Western Hemisphere and the Saharan Air Layer. *Bulletin of the American*
728 *Meteorological Society* **102**, E1239-E1260, doi:10.1175/bams-d-19-0309.1 (2021).
- 729 11 Highwood, E. J. & Ryder, C. L. in *Mineral Dust: A Key Player in the Earth System* (eds
730 Peter Knippertz & Jan-Berend W. Stuut) 327-357 (Springer Netherlands, 2014).
- 731 12 Storelvmo, T. Aerosol Effects on Climate via Mixed-Phase and Ice Clouds. *Annual*
732 *Review of Earth and Planetary Sciences*, Vol 45 **45**, 199-222, doi:10.1146/annurev-earth-
733 060115-012240 (2017).

734 13 Karydis, V. A. *et al.* Global impact of mineral dust on cloud droplet number
735 concentration. *Atmospheric Chemistry and Physics* **17**, 5601-5621, doi:10.5194/acp-17-
736 5601-2017 (2017).

737 14 Klingmuller, K., Karydis, V. A., Bacer, S., Stenchikov, G. L. & Lelieveld, J. Weaker
738 cooling by aerosols due to dust-pollution interactions. *Atmospheric Chemistry and*
739 *Physics* **20**, 15285-15295, doi:10.5194/acp-20-15285-2020 (2020).

740 15 Klingmuller, K., Lelieveld, J., Karydis, V. A. & Stenchikov, G. L. Direct radiative effect
741 of dust-pollution interactions. *Atmospheric Chemistry and Physics* **19**, 7397-7408,
742 doi:10.5194/acp-19-7397-2019 (2019).

743 16 Bauer, S. E. *et al.* Do sulfate and nitrate coatings on mineral dust have important effects
744 on radiative properties and climate modeling? *J. Geophys. Res.-Atmos.* **112**,
745 doi:10.1029/2005jd006977 (2007).

746 17 Usher, C. R., Michel, A. E. & Grassian, V. H. Reactions on mineral dust. *Chemical*
747 *Reviews* **103**, 4883-4939, doi:10.1021/cr020657y (2003).

748 18 Skiles, S. M., Flanner, M., Cook, J. M., Dumont, M. & Painter, T. H. Radiative forcing
749 by light-absorbing particles in snow. *Nature Climate Change* **8**, 965-+,
750 doi:10.1038/s41558-018-0296-5 (2018).

751 19 Tuccella, P., Pitari, G., Colaiuda, V., Raparelli, E. & Curci, G. Present-day radiative
752 effect from radiation-absorbing aerosols in snow. *Atmospheric Chemistry and Physics* **21**,
753 6875-6893, doi:10.5194/acp-21-6875-2021 (2021).

754 20 Mahowald, N. Aerosol Indirect Effect on Biogeochemical Cycles and Climate. *Science*
755 **334**, 794-796, doi:10.1126/science.1207374 (2011).

756 21 McGraw, Z., Storelvmo, T., David, R. O. & Sagoo, N. Global Radiative Impacts of
757 Mineral Dust Perturbations Through Stratiform Clouds. *Journal of Geophysical*
758 *Research-Atmospheres* **125**, doi:10.1029/2019jd031807 (2020).

759 22 Mahowald, N. M. *et al.* Observed 20th century desert dust variability: impact on climate
760 and biogeochemistry. *Atmos. Chem. Phys.* **10**, 10875-10893, doi:10.5194/acp-10-10875-
761 2010 (2010).

762 23 Hooper, J. & Marx, S. A global doubling of dust emissions during the Anthropocene? *Glob.*
763 *Planet. Change* **169**, 70-91, doi:10.1016/j.gloplacha.2018.07.003 (2018).

764 24 Boucher, O. & Tanre, D. Estimation of the aerosol perturbation to the Earth's radiative
765 budget over oceans using POLDER satellite aerosol retrievals. *Geophysical Research*
766 *Letters* **27**, 1103-1106, doi:10.1029/1999gl010963 (2000).

767 25 Boucher, O. *et al.* in *Climate Change 2013: The Physical Science Basis. Contribution of*
768 *Working Group I to the Fifth Assessment Report of the Intergovernmental Panel on*
769 *Climate Change* (eds T.F. Stocker *et al.*) pp. 571–658 (Cambridge University Press,
770 2013).

771 26 Carslaw, K. S. *et al.* Large contribution of natural aerosols to uncertainty in indirect
772 forcing. *Nature* **503**, 67-+, doi:10.1038/nature12674 (2013).

773 27 Forster, P. *et al.* in *Climate Change 2007: The Physical Science Basis.* (ed S. Solomon,
774 D. Qin, M. Manning, Z. Chen, M. Marquis, K.B. Averyt, M.Tignor and H.L. Miller)
775 (Cambridge University Press, 2007).

776 28 Forster, P. *et al.* (eds V. Masson-Delmotte *et al.*) Ch. Chapter 7: The Earth's energy
777 budget, climate feedbacks, and climate sensitivity, (2021).

778 29 Ryder, C. L. *et al.* Optical properties of Saharan dust aerosol and contribution from the
779 coarse mode as measured during the Fennec 2011 aircraft campaign. *Atmospheric
780 Chemistry and Physics* **13**, 303-325, doi:10.5194/acp-13-303-2013 (2013).

781 30 Tegen, I. & Lacis, A. A. Modeling of particle size distribution and its influence on the
782 radiative properties of mineral dust aerosol. *Journal of Geophysical Research-
783 Atmospheres* **101**, 19237-19244 (1996).

784 31 Sokolik, I. N. & Toon, O. B. Incorporation of mineralogical composition into models of
785 the radiative properties of mineral aerosol from UV to IR wavelengths. *Journal of
786 Geophysical Research-Atmospheres* **104**, 9423-9444, doi:10.1029/1998jd200048 (1999).

787 32 Di Biagio, C., Balkanski, Y., Albani, S., Boucher, O. & Formenti, P. Direct Radiative
788 Effect by Mineral Dust Aerosols Constrained by New Microphysical and Spectral Optical
789 Data. *Geophysical Research Letters* **47**, doi:10.1029/2019gl086186 (2020).

790 33 Dufresne, J. L., Gautier, C., Ricchiazzi, P. & Fouquart, Y. Longwave scattering effects of
791 mineral aerosols. *J. Atmos. Sci.* **59**, 1959-1966, doi:10.1175/1520-
792 0469(2002)059<1959:lseoma>2.0.co;2 (2002).

793 34 Bohren, C. F. & Huffman, D. R. *Absorption and Scattering of Light by Small Particles*.
794 (Wiley, 1983).

795 35 Liou, K. N. *An Introduction to Atmospheric Radiation*. Second edn, (Academic Press,
796 2002).

797 36 Adebiyi, A. A. *et al.* A review of coarse mineral dust in the Earth system. *EarthArXiv
798 preprint*, doi:10.31223/X5QD36 (2022).

799 37 Di Biagio, C. *et al.* Complex refractive indices and single-scattering albedo of global dust
800 aerosols in the shortwave spectrum and relationship to size and iron content. *Atmospheric
801 Chemistry and Physics* **19**, 15503-15531, doi:10.5194/acp-19-15503-2019 (2019).

802 38 Riemer, N., Ault, A. P., West, M., Craig, R. L. & Curtis, J. H. Aerosol Mixing State:
803 Measurements, Modeling, and Impacts. *Reviews of Geophysics* **57**, 187-249,
804 doi:10.1029/2018rg000615 (2019).

805 39 Renard, J. B. *et al.* In situ measurements of desert dust particles above the western
806 Mediterranean Sea with the balloon-borne Light Optical Aerosol Counter/sizer (LOAC)
807 during the ChArMEx campaign of summer 2013. *Atmospheric Chemistry and Physics* **18**,
808 3677-3699, doi:10.5194/acp-18-3677-2018 (2018).

809 40 Denjean, C. *et al.* Size distribution and optical properties of African mineral dust after
810 intercontinental transport. *Journal of Geophysical Research-Atmospheres* **121**, 7117-
811 7138, doi:10.1002/2016jd024783 (2016).

812 41 Seinfeld, J. H. *et al.* ACE-ASIA - Regional climatic and atmospheric chemical effects of
813 Asian dust and pollution. *Bull. Am. Meteorol. Soc.* **85**, 367-380, doi:10.1175/bams-85-3-
814 367 (2004).

815 42 Liao, H. & Seinfeld, J. H. Radiative forcing by mineral dust aerosols: sensitivity to key
816 variables. *Journal of Geophysical Research-Atmospheres* **103**, 31637-31645 (1998).

817 43 Clauquin, T., Schulz, M., Balkanski, Y. & Boucher, O. Uncertainties in assessing radiative
818 forcing by mineral dust. *Tellus Ser. B-Chem. Phys. Meteorol.* **50**, 491-505,
819 doi:10.1034/j.1600-0889.1998.t01-2-00007.x (1998).

820 44 Kok, J. F. *et al.* Improved representation of the global dust cycle using observational
821 constraints on dust properties and abundance. *Atmospheric Chemistry and Physics* **21**,
822 8127-8167, doi:10.5194/acp-21-8127-2021 (2021).

823 45 Di Biagio, C. *et al.* Global scale variability of the mineral dust long-wave refractive
824 index: a new dataset of in situ measurements for climate modeling and remote sensing.
825 *Atmospheric Chemistry and Physics* **17**, 1901-1929, doi:10.5194/acp-17-1901-2017
826 (2017).

827 46 Li, L. L. *et al.* Quantifying the range of the dust direct radiative effect due to source
828 mineralogy uncertainty. *Atmospheric Chemistry and Physics* **21**, 3973-4005,
829 doi:10.5194/acp-21-3973-2021 (2021).

830 47 Sicard, M., Bertolin, S., Mallet, M., Dubuisson, P. & Comeron, A. Estimation of mineral
831 dust long-wave radiative forcing: sensitivity study to particle properties and application
832 to real cases in the region of Barcelona. *Atmospheric Chemistry and Physics* **14**, 9213-
833 9231, doi:10.5194/acp-14-9213-2014 (2014).

834 48 Brindley, H. E. & Russell, J. E. An assessment of Saharan dust loading and the
835 corresponding cloud-free longwave direct radiative effect from geostationary satellite
836 observations. *Journal of Geophysical Research-Atmospheres* **114**,
837 doi:10.1029/2008jd011635 (2009).

838 49 Adebiyi, A. A. & Kok, J. F. Climate models miss most of the coarse dust in the
839 atmosphere. *Science Advances* **6**, eaaz9507, doi:10.1126/sciadv.aaz9507 (2020).

840 50 Tuccella, P., Curci, G., Pitari, G., Lee, S. & Jo, D. S. Direct Radiative Effect of
841 Absorbing Aerosols: Sensitivity to Mixing State, Brown Carbon, and Soil Dust
842 Refractive Index and Shape. *Journal of Geophysical Research-Atmospheres* **125**,
843 doi:10.1029/2019jd030967 (2020).

844 51 Albani, S. *et al.* Improved dust representation in the Community Atmosphere Model. *J.
845 Adv. Model. Earth Sy.* **6**, 541-570, doi:10.1002/2013ms000279 (2014).

846 52 Ito, A., Adebiyi, A. A., Huang, Y. & Kok, J. F. Less atmospheric radiative heating by
847 dust due to the synergy of coarser size and aspherical shape. *Atmospheric Chemistry and
848 Physics* **21**, 16869-16891, doi:10.5194/acp-21-16869-2021 (2021).

849 53 Colarco, P. R. *et al.* Impact of radiatively interactive dust aerosols in the NASA GEOS-5
850 climate model: Sensitivity to dust particle shape and refractive index. *Journal of
851 Geophysical Research-Atmospheres* **119**, 753-786, doi:10.1002/2013jd020046 (2014).

852 54 Ryder, C. L. *et al.* Coarse-mode mineral dust size distributions, composition and optical
853 properties from AER-D aircraft measurements over the tropical eastern Atlantic.
854 *Atmospheric Chemistry and Physics* **18**, 17225-17257, doi:10.5194/acp-18-17225-2018
855 (2018).

856 55 Weinzierl, B. *et al.* The Saharan Aerosol Long-range Transport and Aerosol-Cloud
857 Interaction Experiment (SALTRACE): overview and selected highlights. *Bull. Am.
858 Meteorol. Soc.* **98**, 1427-1451, doi:10.1175/BAMS-D-15-00142.1 (2017).

859 56 Ansmann, A. *et al.* Profiling of Saharan dust from the Caribbean to West Africa, Part 2:
860 Shipborne lidar measurements versus forecasts. *Atmospheric Chemistry and Physics
861 Discussions*, doi:10.5194/acp-2017-502 (2017).

862 57 Song, Q. *et al.* Toward an Observation-Based Estimate of Dust Net Radiative Effects in
863 Tropical North Atlantic Through Integrating Satellite Observations and In Situ
864 Measurements of Dust Properties. *Atmos. Chem. Phys. Discuss.* **in review** (2018).

865 58 O'Sullivan, D. *et al.* Models transport Saharan dust too low in the atmosphere: a
866 comparison of the MetUM and CAMS forecasts with observations. *Atmospheric
867 Chemistry and Physics* **20**, 12955-12982, doi:10.5194/acp-20-12955-2020 (2020).

868 59 Kim, D. *et al.* Sources, sinks, and transatlantic transport of North African dust aerosol: A
869 multimodel analysis and comparison with remote sensing data. *Journal of Geophysical*
870 *Research-Atmospheres* **119**, 6259-6277, doi:10.1002/2013jd021099 (2014).

871 60 Karydis, V. A., Tsimpidi, A. P., Lei, W., Molina, L. T. & Pandis, S. N. Formation of
872 semivolatile inorganic aerosols in the Mexico City Metropolitan Area during the
873 MILAGRO campaign. *Atmospheric Chemistry and Physics* **11**, 13305-13323,
874 doi:10.5194/acp-11-13305-2011 (2011).

875 61 Formenti, P., Elbert, W., Maenhaut, W., Haywood, J. & Andreae, M. O. Chemical
876 composition of mineral dust aerosol during the Saharan Dust Experiment (SHADE)
877 airborne campaign in the Cape Verde region, September 2000. *Journal of Geophysical*
878 *Research-Atmospheres* **108**, doi:10.1029/2002jd002648 (2003).

879 62 Begue, N. *et al.* Aerosol processing and CCN formation of an intense Saharan dust plume
880 during the EUCAARI 2008 campaign. *Atmospheric Chemistry and Physics* **15**, 3497-
881 3516, doi:10.5194/acp-15-3497-2015 (2015).

882 63 Li, W. J. & Shao, L. Y. Observation of nitrate coatings on atmospheric mineral dust
883 particles. *Atmospheric Chemistry and Physics* **9**, 1863-1871, doi:10.5194/acp-9-1863-
884 2009 (2009).

885 64 Karydis, V. A., Tsimpidi, A. P., Pozzer, A., Astitha, M. & Lelieveld, J. Effects of mineral
886 dust on global atmospheric nitrate concentrations. *Atmospheric Chemistry and Physics*
887 **16**, 1491-1509, doi:10.5194/acp-16-1491-2016 (2016).

888 65 Sullivan, R. C., Guazzotti, S. A., Sodeman, D. A. & Prather, K. A. Direct observations of
889 the atmospheric processing of Asian mineral dust. *Atmospheric Chemistry and Physics* **7**,
890 1213-1236 (2007).

891 66 Huang, X. *et al.* Pathways of sulfate enhancement by natural and anthropogenic mineral
892 aerosols in China. *Journal of Geophysical Research-Atmospheres* **119**, 14165-14179,
893 doi:10.1002/2014jd022301 (2014).

894 67 Sullivan, R. C. *et al.* Mineral dust is a sink for chlorine in the marine boundary layer.
895 *Atmos. Environ.* **41**, 7166-7179, doi:10.1016/j.atmosenv.2007.05.047 (2007).

896 68 Feng, T. *et al.* Summertime ozone formation in Xi'an and surrounding areas, China.
897 *Atmospheric Chemistry and Physics* **16**, 4323-4342, doi:10.5194/acp-16-4323-2016
898 (2016).

899 69 Gharibzadeh, M., Bidokhti, A. A. & Alam, K. The interaction of ozone and aerosol in a
900 semi-arid region in the Middle East: Ozone formation and radiative forcing implications.
901 *Atmos. Environ.* **245**, doi:10.1016/j.atmosenv.2020.118015 (2021).

902 70 Usher, C. R., Al-Hosney, H., Carlos-Cuellar, S. & Grassian, V. H. A laboratory study of
903 the heterogeneous uptake and oxidation of sulfur dioxide on mineral dust particles.
904 *Journal of Geophysical Research-Atmospheres* **107**, doi:10.1029/2002jd002051 (2002).

905 71 Goodman, A. L., Underwood, G. M. & Grassian, V. H. Heterogeneous reaction of NO₂:
906 Characterization of gas-phase and adsorbed products from the reaction,
907 2NO(2)(g)+H₂O(a)->HONO(g)+HNO₃(a) on hydrated silica particles. *Journal of*
908 *Physical Chemistry A* **103**, 7217-7223, doi:10.1021/jp9910688 (1999).

909 72 Nenes, A., Pandis, S. N., Weber, R. J. & Russell, A. Aerosol pH and liquid water content
910 determine when particulate matter is sensitive to ammonia and nitrate availability.
911 *Atmospheric Chemistry and Physics* **20**, 3249-3258, doi:10.5194/acp-20-3249-2020
912 (2020).

913 73 Karydis, V. A., Tsimpidi, A. P., Pozzer, A. & Lelieveld, J. How alkaline compounds
914 control atmospheric aerosol particle acidity. *Atmospheric Chemistry and Physics* **21**,
915 14983-15001, doi:10.5194/acp-21-14983-2021 (2021).

916 74 Trochkine, D. *et al.* Mineral aerosol particles collected in Dunhuang, China, and their
917 comparison with chemically modified particles collected over Japan. *Journal of*
918 *Geophysical Research-Atmospheres* **108**, doi:10.1029/2002jd003268 (2003).

919 75 Fitzgerald, E., Ault, A. P., Zauscher, M. D., Mayol-Bracero, O. L. & Prather, K. A.
920 Comparison of the mixing state of long-range transported Asian and African mineral
921 dust. *Atmos. Environ.* **115**, 19-25, doi:10.1016/j.atmosenv.2015.04.031 (2015).

922 76 Klingmuller, K. *et al.* Revised mineral dust emissions in the atmospheric chemistry-
923 climate model EMAC (MESSy 2.52 DU_Astitha1 KKDU2017 patch). *Geoscientific*
924 *Model Development* **11**, 989-1008, doi:10.5194/gmd-11-989-2018 (2018).

925 77 Perlitz, J. P., Perez Garcia-Pando, C. & Miller, R. L. Predicting the mineral
926 composition of dust aerosols - Part 1: Representing key processes. *Atmos. Chem. Phys.*
927 **15**, 11593-11627 (2015).

928 78 Sullivan, R. C. *et al.* Effect of chemical mixing state on the hygroscopicity and cloud
929 nucleation properties of calcium mineral dust particles. *Atmospheric Chemistry and*
930 *Physics* **9**, 3303-3316, doi:10.5194/acp-9-3303-2009 (2009).

931 79 Tang, M. J., Cziczo, D. J. & Grassian, V. H. Interactions of Water with Mineral Dust
932 Aerosol: Water Adsorption, Hygroscopicity, Cloud Condensation, and Ice Nucleation.
933 *Chemical Reviews* **116**, 4205-4259, doi:10.1021/acs.chemrev.5b00529 (2016).

934 80 Cziczo, D. J. *et al.* Deactivation of ice nuclei due to atmospherically relevant surface
935 coatings. *Environmental Research Letters* **4**, doi:10.1088/1748-9326/4/4/044013 (2009).

936 81 Fan, S. M., Horowitz, L. W., Levy, H. & Moxim, W. J. Impact of air pollution on wet
937 deposition of mineral dust aerosols. *Geophysical Research Letters* **31**,
938 doi:10.1029/2003gl018501 (2004).

939 82 Liao, H., Seinfeld, J. H., Adams, P. J. & Mickley, L. J. Global radiative forcing of
940 coupled tropospheric ozone and aerosols in a unified general circulation model. *Journal*
941 *of Geophysical Research-Atmospheres* **109**, D16207, doi:10.1029/2003jd004456 (2004).

942 83 Bauer, S. E. & Koch, D. Impact of heterogeneous sulfate formation at mineral dust
943 surfaces on aerosol loads and radiative forcing in the Goddard Institute for Space Studies
944 general circulation model. *Journal of Geophysical Research-Atmospheres* **110**,
945 doi:10.1029/2005jd005870 (2005).

946 84 Koehler, K. A. *et al.* Hygroscopicity and cloud droplet activation of mineral dust aerosol.
947 *Geophysical Research Letters* **36**, doi:10.1029/2009gl037348 (2009).

948 85 Kumar, P., Sokolik, I. N. & Nenes, A. Measurements of cloud condensation nuclei
949 activity and droplet activation kinetics of fresh unprocessed regional dust samples and
950 minerals. *Atmospheric Chemistry and Physics* **11**, 3527-3541, doi:10.5194/acp-11-3527-
951 2011 (2011).

952 86 Gaston, C. J. Re-examining Dust Chemical Aging and Its Impacts on Earth's Climate.
953 *Accounts of Chemical Research* **53**, 1005-1013, doi:10.1021/acs.accounts.0c00102
954 (2020).

955 87 Karydis, V. A., Kumar, P., Barahona, D., Sokolik, I. N. & Nenes, A. On the effect of dust
956 particles on global cloud condensation nuclei and cloud droplet number. *Journal of*
957 *Geophysical Research-Atmospheres* **116**, doi:10.1029/2011jd016283 (2011).

958 88 Sagoo, N. & Storelvmo, T. Testing the sensitivity of past climates to the indirect effects
959 of dust. *Geophysical Research Letters* **44**, 5807-5817, doi:10.1002/2017gl072584 (2017).
960 89 Li, R., Min, Q. L. & Harrison, L. C. A Case Study: The Indirect Aerosol Effects of
961 Mineral Dust on Warm Clouds. *J. Atmos. Sci.* **67**, 805-816, doi:10.1175/2009jas3235.1
962 (2010).
963 90 Hoose, C. & Mohler, O. Heterogeneous ice nucleation on atmospheric aerosols: a review
964 of results from laboratory experiments. *Atmospheric Chemistry and Physics* **12**, 9817-
965 9854, doi:10.5194/acp-12-9817-2012 (2012).
966 91 Kanji, Z. A. *et al.* Overview of Ice Nucleating Particles. *Ice Formation and Evolution in
967 Clouds and Precipitation: Measurement and Modeling Challenges* **58**,
968 doi:10.1175/amsmonographs-d-16-0006.1 (2017).
969 92 David, R. O. *et al.* Pore condensation and freezing is responsible for ice formation below
970 water saturation for porous particles. *Proc. Natl. Acad. Sci. U. S. A.* **116**, 8184-8189,
971 doi:10.1073/pnas.1813647116 (2019).
972 93 Matus, A. V. & L'Ecuyer, T. S. The role of cloud phase in Earth's radiation budget.
973 *Journal of Geophysical Research-Atmospheres* **122**, 2559-2578,
974 doi:10.1002/2016jd025951 (2017).
975 94 Morrison, H. *et al.* Resilience of persistent Arctic mixed-phase clouds. *Nature
976 Geoscience* **5**, 11-17, doi:10.1038/ngeo1332 (2012).
977 95 Shi, Y. & Liu, X. H. Dust Radiative Effects on Climate by Glaciating Mixed-Phase
978 Clouds. *Geophysical Research Letters* **46**, 6128-6137, doi:10.1029/2019gl082504 (2019).
979 96 Choi, Y. S., Lindzen, R. S., Ho, C. H. & Kim, J. Space observations of cold-cloud phase
980 change. *Proc. Natl. Acad. Sci. U. S. A.* **107**, 11211-11216, doi:10.1073/pnas.1006241107
981 (2010).
982 97 Tan, I., Storelvmo, T. & Choi, Y. S. Spaceborne lidar observations of the ice-nucleating
983 potential of dust, polluted dust, and smoke aerosols in mixed-phase clouds. *Journal of
984 Geophysical Research-Atmospheres* **119**, 6653-6665, doi:10.1002/2013jd021333 (2014).
985 98 Froyd, K. D. *et al.* Dominant role of mineral dust in cirrus cloud formation revealed by
986 global-scale measurements. *Nature Geoscience* **15**, 177-+, doi:10.1038/s41561-022-
987 00901-w (2022).
988 99 Cziczo, D. J. *et al.* Clarifying the Dominant Sources and Mechanisms of Cirrus Cloud
989 Formation. *Science* **340**, 1320-1324, doi:10.1126/science.1234145 (2013).
990 100 Heymsfield, A. J. *et al.* Cirrus Clouds. *Ice Formation and Evolution in Clouds and
991 Precipitation: Measurement and Modeling Challenges* **58**, doi:10.1175/amsmonographs-
992 d-16-0010.1 (2017).
993 101 Storelvmo, T. & Herger, N. Cirrus cloud susceptibility to the injection of ice nuclei in the
994 upper troposphere. *Journal of Geophysical Research-Atmospheres* **119**, 2375-2389,
995 doi:10.1002/2013jd020816 (2014).
996 102 DeMott, P. J. *et al.* Integrating laboratory and field data to quantify the immersion
997 freezing ice nucleation activity of mineral dust particles. *Atmospheric Chemistry and
998 Physics* **15**, 393-409, doi:10.5194/acp-15-393-2015 (2015).
999 103 Ullrich, R. *et al.* A New Ice Nucleation Active Site Parameterization for Desert Dust and
1000 Soot. *J. Atmos. Sci.* **74**, 699-717, doi:10.1175/jas-d-16-0074.1 (2017).
1001 104 Liu, X. *et al.* Sensitivity studies of dust ice nuclei effect on cirrus clouds with the
1002 Community Atmosphere Model CAM5. *Atmospheric Chemistry and Physics* **12**, 12061-
1003 12079, doi:10.5194/acp-12-12061-2012 (2012).

1004 105 Huang, J. P., Wang, T. H., Wang, W. C., Li, Z. Q. & Yan, H. R. Climate effects of dust
1005 aerosols over East Asian arid and semiarid regions. *Journal of Geophysical Research-Atmospheres* **119**, 11398-11416, doi:10.1002/2014jd021796 (2014).

1006 106 Perlitz, J. & Miller, R. L. Cloud cover increase with increasing aerosol absorptivity: A
1007 counterexample to the conventional semidirect aerosol effect. *Journal of Geophysical
1008 Research-Atmospheres* **115**, doi:10.1029/2009jd012637 (2010).

1009 107 Amiri-Farahani, A., Allen, R. J., Neubauer, D. & Lohmann, U. Impact of Saharan dust on
1010 North Atlantic marine stratocumulus clouds: importance of the semidirect effect.
1011 *Atmospheric Chemistry and Physics* **17**, 6305-6322, doi:10.5194/acp-17-6305-2017
1012 (2017).

1013 108 DeFlorio, M. J. *et al.* Semidirect dynamical and radiative effect of North African dust
1014 transport on lower tropospheric clouds over the subtropical North Atlantic in CESM 1.0.
1015 *Journal of Geophysical Research-Atmospheres* **119**, doi:10.1002/2013jd020997 (2014).

1016 109 Hansen, J., Sato, M. & Ruedy, R. Radiative forcing and climate response. *Journal of
1017 Geophysical Research-Atmospheres* **102**, 6831-6864, doi:10.1029/96jd03436 (1997).

1018 110 Ackerman, A. S. *et al.* Reduction of tropical cloudiness by soot. *Science* **288**, 1042-1047,
1019 doi:10.1126/science.288.5468.1042 (2000).

1020 111 Sand, M. *et al.* Aerosol absorption in global models from AeroCom phase III.
1021 *Atmospheric Chemistry and Physics* **21**, 15929-15947, doi:10.5194/acp-21-15929-2021
1022 (2021).

1023 112 Samset, B. H. *et al.* Aerosol Absorption: Progress Towards Global and Regional
1024 Constraints. *Current Climate Change Reports* **4**, 65-83 (2018).

1025 113 Russell, P. B. *et al.* Absorption Angstrom Exponent in AERONET and related data as an
1026 indicator of aerosol composition. *Atmospheric Chemistry and Physics* **10**, 1155-1169,
1027 doi:10.5194/acp-10-1155-2010 (2010).

1028 114 Koch, D. & Del Genio, A. D. Black carbon semi-direct effects on cloud cover: review
1029 and synthesis. *Atmospheric Chemistry and Physics* **10**, 7685-7696, doi:10.5194/acp-10-
1030 7685-2010 (2010).

1031 115 Doherty, O. M. & Evan, A. T. Identification of a new dust-stratocumulus indirect effect
1032 over the tropical North Atlantic. *Geophysical Research Letters* **41**, 6935-6942,
1033 doi:10.1002/2014gl060897 (2014).

1034 116 Huang, J. P. *et al.* Satellite-based assessment of possible dust aerosols semi-direct effect
1035 on cloud water path over East Asia. *Geophysical Research Letters* **33**,
1036 doi:10.1029/2006gl026561 (2006).

1037 117 McFarquhar, G. M. & Wang, H. L. Effects of aerosols on trade wind cumuli over the
1038 Indian Ocean: Model simulations. *Quarterly Journal of the Royal Meteorological Society*
1039 **132**, 821-843, doi:10.1256/qj.04.179 (2006).

1040 118 Feingold, G., Jiang, H. L. & Harrington, J. Y. On smoke suppression of clouds in
1041 Amazonia. *Geophysical Research Letters* **32**, doi:10.1029/2004gl021369 (2005).

1042 119 Stephens, G. L., Wood, N. B. & Pakula, L. A. On the radiative effects of dust on tropical
1043 convection. *Geophysical Research Letters* **31**, doi:10.1029/2004gl021342 (2004).

1044 120 Miller, R. L., Tegen, I. & Perlitz, J. Surface radiative forcing by soil dust aerosols and
1045 the hydrologic cycle. *Journal of Geophysical Research-Atmospheres* **109**, D04203,
1046 doi:10.1029/2003jd004085 (2004).

1047

1048 121 Wong, S., Dessler, A. E., Mahowald, N. M., Yang, P. & Feng, Q. Maintenance of Lower
1049 Tropospheric Temperature Inversion in the Saharan Air Layer by Dust and Dry Anomaly.
1050 *Journal of Climate* **22**, 5149-5162, doi:10.1175/2009jcli2847.1 (2009).

1051 122 Zhu, A., Ramanathan, V., Li, F. & Kim, D. Dust plumes over the Pacific, Indian, and
1052 Atlantic oceans: Climatology and radiative impact. *Journal of Geophysical Research-
1053 Atmospheres* **112**, doi:10.1029/2007jd008427 (2007).

1054 123 Chen, S. H., Wang, S. H. & Waylonis, M. Modification of Saharan air layer and
1055 environmental shear over the eastern Atlantic Ocean by dust-radiation effects. *Journal of
1056 Geophysical Research-Atmospheres* **115**, D21202, doi:D2120210.1029/2010jd014158
1057 (2010).

1058 124 Ryder, C. L. *et al.* Coarse and giant particles are ubiquitous in Saharan dust export
1059 regions and are radiatively significant over the Sahara. *Atmospheric Chemistry and
1060 Physics* **19**, 15353-15376, doi:10.5194/acp-19-15353-2019 (2019).

1061 125 Huang, J. P. *et al.* Possible influences of Asian dust aerosols on cloud properties and
1062 radiative forcing observed from MODIS and CERES. *Geophysical Research Letters* **33**,
1063 doi:10.1029/2005gl024724 (2006).

1064 126 Amiri-Farahani, A., Allen, R. J., Li, K. F. & Chu, J. E. The Semidirect Effect of
1065 Combined Dust and Sea Salt Aerosols in a Multimodel Analysis. *Geophysical Research
1066 Letters* **46**, 10512-10521, doi:10.1029/2019gl084590 (2019).

1067 127 Tegen, I. & Heinold, B. Large-Scale Modeling of Absorbing Aerosols and Their Semi-
1068 Direct Effects. *Atmosphere* **9**, doi:10.3390/atmos9100380 (2018).

1069 128 Painter, T. H. *et al.* Response of Colorado River runoff to dust radiative forcing in snow.
1070 *Proc. Natl. Acad. Sci. U. S. A.* **107**, 17125-17130, doi:10.1073/pnas.0913139107 (2010).

1071 129 Lee, W. L. *et al.* Impact of absorbing aerosol deposition on snow albedo reduction over
1072 the southern Tibetan plateau based on satellite observations. *Theoretical and Applied
1073 Climatology* **129**, 1373-1382, doi:10.1007/s00704-016-1860-4 (2017).

1074 130 Hall, A. The role of surface albedo feedback in climate. *Journal of Climate* **17**, 1550-
1075 1568, doi:10.1175/1520-0442(2004)017<1550:trosaf>2.0.co;2 (2004).

1076 131 Flanner, M. G. *et al.* Springtime warming and reduced snow cover from carbonaceous
1077 particles. *Atmospheric Chemistry and Physics* **9**, 2481-2497 (2009).

1078 132 Dang, C., Brandt, R. E. & Warren, S. G. Parameterizations for narrowband and
1079 broadband albedo of pure snow and snow containing mineral dust and black carbon.
1080 *Journal of Geophysical Research-Atmospheres* **120**, 5446-5468,
1081 doi:10.1002/2014jd022646 (2015).

1082 133 Flanner, M. G. *et al.* SNICAR-ADv3: a community tool for modeling spectral snow
1083 albedo. *Geoscientific Model Development* **14**, 7673-7704, doi:10.5194/gmd-14-7673-
1084 2021 (2021).

1085 134 Liou, K. N. *et al.* Stochastic parameterization for light absorption by internally mixed
1086 BC/dust in snow grains for application to climate models. *Journal of Geophysical
1087 Research-Atmospheres* **119**, 7616-7632, doi:10.1002/2014jd021665 (2014).

1088 135 He, C. L., Liou, K. N., Takano, Y., Chen, F. & Barlage, M. Enhanced Snow Absorption
1089 and Albedo Reduction by Dust-Snow Internal Mixing: Modeling and Parameterization. *J.
1090 Adv. Model. Earth Syst.* **11**, 3755-3776, doi:10.1029/2019ms001737 (2019).

1091 136 Warren, S. G. & Wiscombe, W. J. A Model For The Spectral Albedo Of Snow .2. Snow
1092 Containing Atmospheric Aerosols. *J. Atmos. Sci.* **37**, 2734-2745, doi:10.1175/1520-
1093 0469(1980)037<2734:amftsa>2.0.co;2 (1980).

1094 137 He, C., Takano, Y. & Liou, K. N. Close packing effects on clean and dirty snow albedo
1095 and associated climatic implications. *Geophysical Research Letters* **44**, 3719-3727,
1096 doi:10.1002/2017gl072916 (2017).

1097 138 He, C. & Flanner, M. Snow Albedo and Radiative Transfer: Theory, Modeling, and
1098 Parameterization. *Springer Series in Light Scattering, Vol 5: Radiative Transfer, Remote*
1099 *Sensing, and Light Scattering*, 67-133, doi:10.1007/978-3-030-38696-2_3 (2020).

1100 139 Dang, C. *et al.* Measurements of light-absorbing particles in snow across the Arctic,
1101 North America, and China: Effects on surface albedo. *Journal of Geophysical Research-Atmospheres* **122**,
1102 10149-10168, doi:10.1002/2017jd027070 (2017).

1103 140 Kylling, A., Zwaafink, C. D. G. & Stohl, A. Mineral Dust Instantaneous Radiative
1104 Forcing in the Arctic. *Geophysical Research Letters* **45**, 4290-4298,
1105 doi:10.1029/2018gl077346 (2018).

1106 141 Dong, Z. W. *et al.* Aeolian dust transport, cycle and influences in high-elevation
1107 cryosphere of the Tibetan Plateau region: New evidences from alpine snow and ice.
1108 *Earth-Sci. Rev.* **211**, doi:10.1016/j.earscirev.2020.103408 (2020).

1109 142 Di Mauro, B. *et al.* Mineral dust impact on snow radiative properties in the European
1110 Alps combining ground, UAV, and satellite observations. *Journal of Geophysical*
1111 *Research-Atmospheres* **120**, 6080-6097, doi:10.1002/2015jd023287 (2015).

1112 143 Skiles, S. M. & Painter, T. H. Toward Understanding Direct Absorption and Grain Size
1113 Feedbacks by Dust Radiative Forcing in Snow With Coupled Snow Physical and
1114 Radiative Transfer Modeling. *Water Resour. Res.* **55**, 7362-7378,
1115 doi:10.1029/2018wr024573 (2019).

1116 144 Lawrence, D. M. *et al.* The CCSM4 Land Simulation, 1850-2005: Assessment of Surface
1117 Climate and New Capabilities. *Journal of Climate* **25**, 2240-2260, doi:10.1175/jcli-d-11-
1118 00103.1 (2012).

1119 145 Martin, J. H. Glacial-interglacial CO₂ change: The iron hypothesis. *Paleoceanography* **5**,
1120 1-13, doi:10.1029/PA005i001p00001 (1990).

1121 146 Moore, C. M. *et al.* Processes and patterns of oceanic nutrient limitation. *Nature Geoscience* **6**,
1122 701-710, doi:10.1038/ngeo1765 (2013).

1123 147 Capone, D. G., Zehr, J. P., Paerl, H. W., Bergman, B. & Carpenter, E. J. *Trichodesmium*,
1124 a globally significant marine cyanobacterium. *Science* **276**, 1221-1229,
1125 doi:10.1126/science.276.5316.1221 (1997).

1126 148 Moore, J. K., Doney, S. C., Lindsay, K., Mahowald, N. & Michaels, A. F. Nitrogen
1127 fixation amplifies the ocean biogeochemical response to decadal timescale variations in
1128 mineral dust deposition. *Tellus Ser. B-Chem. Phys. Meteorol.* **58**, 560-572,
1129 doi:10.1111/j.1600-0889.2006.00209.x (2006).

1130 149 Fung, I. Y. *et al.* Iron supply and demand in the upper ocean. *Global Biogeochemical*
1131 *Cycles* **14**, 281-295, doi:10.1029/1999gb900059 (2000).

1132 150 Lam, P. J. & Bishop, J. K. B. The continental margin is a key source of iron to the HNLC
1133 North Pacific Ocean. *Geophysical Research Letters* **35**, doi:10.1029/2008gl033294
1134 (2008).

1135 151 Moore, J. K. & Braucher, O. Sedimentary and mineral dust sources of dissolved iron to
1136 the world ocean. *Biogeosciences* **5**, 631-656, doi:10.5194/bg-5-631-2008 (2008).

1137 152 Parekh, P., Follows, M. J. & Boyle, E. Modeling the global ocean iron cycle. *Global*
1138 *Biogeochemical Cycles* **18**, doi:10.1029/2003gb002061 (2004).

1139 153 Mahowald, N. M. *et al.* Aerosol trace metal leaching and impacts on marine
1140 microorganisms. *Nature Communications* **9**, doi:10.1038/s41467-018-04970-7 (2018).
1141 154 Johnson, M. S. & Meskhidze, N. Atmospheric dissolved iron deposition to the global
1142 oceans: effects of oxalate-promoted Fe dissolution, photochemical redox cycling, and
1143 dust mineralogy. *Geoscientific Model Development* **6**, 1137-1155, doi:10.5194/gmd-6-
1144 1137-2013 (2013).
1145 155 Meskhidze, N., Chameides, W. L. & Nenes, A. Dust and pollution: A recipe for enhanced
1146 ocean fertilization? *Journal of Geophysical Research-Atmospheres* **110**,
1147 doi:10.1029/2004jd005082 (2005).
1148 156 Chuang, P. Y., Duvall, R. M., Shafer, M. M. & Schauer, J. J. The origin of water soluble
1149 particulate iron in the Asian atmospheric outflow. *Geophysical Research Letters* **32**,
1150 doi:10.1029/2004gl021946 (2005).
1151 157 Guieu, C., Bonnet, S., Wagener, T. & Loyer-Pilot, M. D. Biomass burning as a source of
1152 dissolved iron to the open ocean? *Geophysical Research Letters* **32**,
1153 doi:10.1029/2005gl022962 (2005).
1154 158 Tagliabue, A. *et al.* The integral role of iron in ocean biogeochemistry. *Nature* **543**, 51-
1155 59, doi:10.1038/nature21058 (2017).
1156 159 Krishnamurthy, A., Moore, J. K., Mahowald, N., Luo, C. & Zender, C. S. Impacts of
1157 atmospheric nutrient inputs on marine biogeochemistry. *Journal of Geophysical
1158 Research-Biogeosciences* **115**, doi:10.1029/2009jg001115 (2010).
1159 160 Mahowald, N. *et al.* Desert dust and anthropogenic aerosol interactions in the
1160 Community Climate System Model coupled-carbon-climate model. *Biogeosciences* **8**,
1161 387-414, doi:10.5194/bg-8-387-2011 (2011).
1162 161 Okin, G. S. *et al.* Spatial patterns of soil nutrients in two southern African savannas.
1163 *Journal of Geophysical Research-Biogeosciences* **113**, doi:10.1029/2007jg000584
1164 (2008).
1165 162 Vitousek, P. M. Litterfall, nutrient cycling, and nutrient limitation in tropical forests.
1166 *Ecology* **65**, 285-298, doi:10.2307/1939481 (1984).
1167 163 Falkowski, P. G., Barber, R. T. & Smetacek, V. Biogeochemical controls and feedbacks
1168 on ocean primary production. *Science* **281**, 200-206, doi:10.1126/science.281.5374.200
1169 (1998).
1170 164 Swap, R., Garstang, M., Greco, S., Talbot, R. & Kallberg, P. Saharan dust in the amazon
1171 basin. *Tellus Ser. B-Chem. Phys. Meteorol.* **44**, 133-149, doi:10.1034/j.1600-
1172 0889.1992.t01-1-00005.x (1992).
1173 165 Okin, G. S., Mahowald, N., Chadwick, O. A. & Artaxo, P. Impact of desert dust on the
1174 biogeochemistry of phosphorus in terrestrial ecosystems. *Global Biogeochemical Cycles*
1175 **18**, Gb2005, doi:10.1029/2003gb002145 (2004).
1176 166 Barkley, A. E. *et al.* African biomass burning is a substantial source of phosphorus
1177 deposition to the Amazon, Tropical Atlantic Ocean, and Southern Ocean. *Proc. Natl.
1178 Acad. Sci. U. S. A.* **116**, 16216-16221, doi:10.1073/pnas.1906091116 (2019).
1179 167 Mahowald, N. M. *et al.* Impacts of biomass burning emissions and land use change on
1180 Amazonian atmospheric phosphorus cycling and deposition. *Global Biogeochemical
1181 Cycles* **19**, doi:10.1029/2005gb002541 (2005).
1182 168 Okin, G. S. *et al.* Impacts of atmospheric nutrient deposition on marine productivity:
1183 Roles of nitrogen, phosphorus, and iron. *Global Biogeochemical Cycles* **25**,
1184 doi:10.1029/2010gb003858 (2011).

1185 169 McConnell, J. R., Aristarain, A. J., Banta, J. R., Edwards, P. R. & Simoes, J. C. 20th-
1186 Century doubling in dust archived in an Antarctic Peninsula ice core parallels climate
1187 change and desertification in South America. *Proc. Natl. Acad. Sci. U. S. A.* **104**, 5743-
1188 5748, doi:10.1073/pnas.0607657104 (2007).

1189 170 Armstrong, R. A., Lee, C., Hedges, J. I., Honjo, S. & Wakeham, S. G. A new,
1190 mechanistic model for organic carbon fluxes in the ocean based on the quantitative
1191 association of POC with ballast minerals. *Deep-Sea Res. Part II-Top. Stud. Oceanogr.* **49**,
1192 219-236, doi:10.1016/s0967-0645(01)00101-1 (2001).

1193 171 van der Jagt, H., Friese, C., Stuut, J. B. W., Fischer, G. & Iversen, M. H. The ballasting
1194 effect of Saharan dust deposition on aggregate dynamics and carbon export: Aggregation,
1195 settling, and scavenging potential of marine snow. *Limnology and Oceanography* **63**,
1196 1386-1394, doi:10.1002/lo.10779 (2018).

1197 172 Paytan, A. *et al.* Toxicity of atmospheric aerosols on marine phytoplankton. *Proc. Natl.*
1198 *Acad. Sci. U. S. A.* **106**, 4601-4605, doi:10.1073/pnas.0811486106 (2009).

1199 173 Thornhill, G. D. *et al.* Effective radiative forcing from emissions of reactive gases and
1200 aerosols - a multi-model comparison. *Atmospheric Chemistry and Physics* **21**, 853-874,
1201 doi:10.5194/acp-21-853-2021 (2021).

1202 174 Patadia, F., Yang, E. S. & Christopher, S. A. Does dust change the clear sky top of
1203 atmosphere shortwave flux over high surface reflectance regions? *Geophysical Research*
1204 *Letters* **36**, L15825, doi:10.1029/2009gl039092 (2009).

1205 175 Jin, Z. H., Charlock, T. P., Smith, W. L. & Rutledge, K. A parameterization of ocean
1206 surface albedo. *Geophysical Research Letters* **31**, doi:10.1029/2004gl021180 (2004).

1207 176 Mulitza, S. *et al.* Increase in African dust flux at the onset of commercial agriculture in
1208 the Sahel region. *Nature* **466**, 226-228, doi:10.1038/nature09213 (2010).

1209 177 Clifford, H. M. *et al.* A 2000 Year Saharan Dust Event Proxy Record from an Ice Core in
1210 the European Alps. *Journal of Geophysical Research-Atmospheres* **124**, 12882-12900,
1211 doi:10.1029/2019jd030725 (2019).

1212 178 Prospero, J. M. & Lamb, P. J. African droughts and dust transport to the Caribbean:
1213 Climate change implications. *Science* **302**, 1024-1027 (2003).

1214 179 Evan, A. T. & Mukhopadhyay, S. African Dust over the Northern Tropical Atlantic:
1215 1955-2008. *Journal of Applied Meteorology and Climatology* **49**, 2213-2229,
1216 doi:10.1175/2010jamc2485.1 (2010).

1217 180 Evan, A. T., Flamant, C., Gaetani, M. & Guichard, F. The past, present and future of
1218 African dust. *Nature* **531**, 493-495 (2016).

1219 181 Mahowald, N. M., Ballantine, J. A., Feddema, J. & Ramankutty, N. Global trends in
1220 visibility: implications for dust sources. *Atmospheric Chemistry and Physics* **7**, 3309-
1221 3339 (2007).

1222 182 Shao, Y. P., Klose, M. & Wyrwoll, K. H. Recent global dust trend and connections to
1223 climate forcing. *Journal of Geophysical Research-Atmospheres* **118**, 11107-11118,
1224 doi:10.1002/jgrd.50836 (2013).

1225 183 Wang, X., Huang, J. P., Ji, M. X. & Higuchi, K. Variability of East Asia dust events and
1226 their long-term trend. *Atmos. Environ.* **42**, 3156-3165,
1227 doi:10.1016/j.atmosenv.2007.07.046 (2008).

1228 184 Zuidema, P. *et al.* Is Summer African Dust Arriving Earlier to Barbados? The Updated
1229 Long-Term In Situ Dust Mass Concentration Time Series from Ragged Point, Barbados,

1230 and Miami, Florida. *Bulletin of the American Meteorological Society* **100**, 1981-1986,
1231 doi:10.1175/bams-d-18-0083.1 (2019).

1232 185 Gkikas, A. *et al.* Quantification of the dust optical depth across spatiotemporal scales
1233 with the MIDAS global dataset (2003-2017). *Atmospheric Chemistry and Physics* **22**,
1234 3553-3578, doi:10.5194/acp-22-3553-2022 (2022).

1235 186 Eyring, V. *et al.* Overview of the Coupled Model Intercomparison Project Phase 6
1236 (CMIP6) experimental design and organization. *Geoscientific Model Development* **9**,
1237 1937-1958, doi:10.5194/gmd-9-1937-2016 (2016).

1238 187 Thornhill, G. *et al.* Climate-driven chemistry and aerosol feedbacks in CMIP6 Earth
1239 system models. *Atmospheric Chemistry and Physics* **21**, 1105-1126, doi:10.5194/acp-21-
1240 1105-2021 (2021).

1241 188 Ginoux, P. *et al.* Sources and distributions of dust aerosols simulated with the GOCART
1242 model. *J. Geophys. Res.* **106**, 20255-20273 (2001).

1243 189 Wu, C. C., Lin, Z. & Liu, X. The global dust cycle and uncertainty in CMIP5 (Coupled
1244 Model Intercomparison Project phase 5) models. *Atmospheric Chemistry and Physics* **20**,
1245 10401-10425, doi:10.5194/acp-20-10401-2020 (2020).

1246 190 Kok, J. F., Albani, S., Mahowald, N. M. & Ward, D. S. An improved dust emission
1247 model - Part 2: Evaluation in the Community Earth System Model, with implications for
1248 the use of dust source functions. *Atmos. Chem. Phys.* **14**, 13043-13061, doi:10.5194/acp-
1249 14-13043-2014 (2014).

1250 191 Ginoux, P., Prospero, J. M., Gill, T. E., Hsu, N. C. & Zhao, M. Global-scale attribution of
1251 anthropogenic and natural dust sources and their emission rates based on MODIS Deep
1252 Blue aerosol products. *Reviews of Geophysics* **50**, Rg3005, doi:10.1029/2012rg000388
1253 (2012).

1254 192 Stevens, B. Rethinking the Lower Bound on Aerosol Radiative Forcing. *J. Climate* **28**,
1255 4794-4819, doi:10.1175/jcli-d-14-00656.1 (2015).

1256 193 Murray, B. J., Carslaw, K. S. & Field, P. R. Opinion: Cloud-phase climate feedback and
1257 the importance of ice-nucleating particles. *Atmospheric Chemistry and Physics* **21**, 665-
1258 679, doi:10.5194/acp-21-665-2021 (2021).

1259 194 Shi, Y. *et al.* Relative importance of high-latitude local and long-range-transported dust
1260 for Arctic ice-nucleating particles and impacts on Arctic mixed-phase clouds.
1261 *Atmospheric Chemistry and Physics* **22**, 2909-2935, doi:10.5194/acp-22-2909-2022
1262 (2022).

1263 195 Andreae, M. O., Jones, C. D. & Cox, P. M. Strong present-day aerosol cooling implies a
1264 hot future. *Nature* **435**, 1187-1190, doi:10.1038/nature03671 (2005).

1265 196 Sherwood, S. C. *et al.* An Assessment of Earth's Climate Sensitivity Using Multiple
1266 Lines of Evidence. *Reviews of Geophysics* **58**, doi:10.1029/2019rg000678 (2020).

1267 197 Caretta, M. A. *et al.* in *Climate Change 2022: Impacts, Adaptation, and Vulnerability.*
1268 *Contribution of Working Group II to the Sixth Assessment Report of the*
1269 *Intergovernmental Panel on Climate Change.* (eds H.-O. Pörtner *et al.*) (Cambridge
1270 University Press, 2022).

1271 198 Cook, B. I. *et al.* Twenty-First Century Drought Projections in the CMIP6 Forcing
1272 Scenarios. *Earth Future* **8**, doi:10.1029/2019ef001461 (2020).

1273 199 Mahowald, N. M. & Luo, C. A less dusty future? *Geophysical Research Letters* **30**, 1903,
1274 doi:10.1029/2003gl017880 (2003).

1275 200 Smith, W. K. *et al.* Large divergence of satellite and Earth system model estimates of
1276 global terrestrial CO₂ fertilization. *Nature Climate Change* **6**, 306-310,
1277 doi:10.1038/nclimate2879 (2016).

1278 201 McVicar, T. R. *et al.* Global review and synthesis of trends in observed terrestrial near-
1279 surface wind speeds: Implications for evaporation. *J. Hydrol.* **416**, 182-205,
1280 doi:10.1016/j.jhydrol.2011.10.024 (2012).

1281 202 Zha, J. L. *et al.* Projected changes in global terrestrial near-surface wind speed in 1.5
1282 degrees C-4.0 degrees C global warming levels. *Environmental Research Letters* **16**,
1283 doi:10.1088/1748-9326/ac2fdd (2021).

1284 203 Pendergrass, A. G., Knutti, R., Lehner, F., Deser, C. & Sanderson, B. M. Precipitation
1285 variability increases in a warmer climate. *Scientific Reports* **7**, doi:10.1038/s41598-017-
1286 17966-y (2017).

1287 204 O'Gorman, P. A. & Schneider, T. The physical basis for increases in precipitation
1288 extremes in simulations of 21st-century climate change. *Proc. Natl. Acad. Sci. U. S. A.*
1289 **106**, 14773-14777, doi:10.1073/pnas.0907610106 (2009).

1290 205 Zender, C. S. & Kwon, E. Y. Regional contrasts in dust emission responses to climate.
1291 *Journal of Geophysical Research-Atmospheres* **110**, doi:10.1029/2004jd005501 (2005).

1292 206 Rodriguez-Caballero, E. *et al.* Global cycling and climate effects of aeolian dust
1293 controlled by biological soil crusts. *Nature Geoscience* **15**, 458-+, doi:10.1038/s41561-
1294 022-00942-1 (2022).

1295 207 Tegen, I., Werner, M., Harrison, S. P. & Kohfeld, K. E. Relative importance of climate
1296 and land use in determining present and future global soil dust emission. *Geophysical
1297 Research Letters* **31**, doi:10.1029/2003gl019216 (2004).

1298 208 Woodward, S., Roberts, D. L. & Betts, R. A. A simulation of the effect of climate
1299 change-induced desertification on mineral dust aerosol. *Geophysical Research Letters* **32**,
1300 L18810, doi:10.1029/2005gl023482 (2005).

1301 209 Mahowald, N. M. *et al.* Change in atmospheric mineral aerosols in response to climate:
1302 Last glacial period, preindustrial, modern, and doubled carbon dioxide climates. *J.
1303 Geophys. Res.* **111**, D10202, doi:10.1029/2005jd006653 (2006).

1304 210 Evan, A. T., Flamant, C., Fiedler, S. & Doherty, O. An analysis of aeolian dust in climate
1305 models. *Geophys. Res. Lett.* **41**, 5996-6001, doi:10.1002/2014GL060545 (2014).

1306 211 Evan, A. T. Surface Winds and Dust Biases in Climate Models. *Geophysical Research
1307 Letters* **45**, 1079-1085, doi:10.1002/2017gl076353 (2018).

1308 212 Wu, C. L. *et al.* Can Climate Models Reproduce the Decadal Change of Dust Aerosol in
1309 East Asia? *Geophysical Research Letters* **45**, 9953-9962, doi:10.1029/2018gl079376
1310 (2018).

1311 213 Pu, B. & Ginoux, P. How reliable are CMIP5 models in simulating dust optical depth?
1312 *Atmospheric Chemistry and Physics* **18**, 12491-12510, doi:10.5194/acp-18-12491-2018
1313 (2018).

1314 214 Zhao, A., Ryder, C. L. & Wilcox, L. J. How well do the CMIP6 models simulate dust
1315 aerosols? *Atmospheric Chemistry and Physics* **22**, 2095-2119, doi:10.5194/acp-22-2095-
1316 2022 (2022).

1317 215 Heinold, B. *et al.* The role of deep convection and nocturnal low-level jets for dust
1318 emission in summertime West Africa: Estimates from convection-permitting simulations.
1319 *Journal of Geophysical Research-Atmospheres* **118**, 4385-4400, doi:10.1002/jgrd.50402
1320 (2013).

1321 216 Kok, J. F., Ward, D. S., Mahowald, N. M. & Evan, A. T. Global and regional importance
1322 of the direct dust-climate feedback. *Nature Communications* **9**, doi:10.1038/s41467-017-
1323 02620-y (2018).

1324 217 Kok, J. F. *et al.* An improved dust emission model - Part 1: Model description and
1325 comparison against measurements. *Atmos. Chem. Phys.* **14**, 13023-13041,
1326 doi:10.5194/acp-14-13023-2014 (2014).

1327 218 Green, R. O. *et al.* in *IEEE Aerospace Conference*. (2020).

1328 219 National Academies of Sciences, E., and Medicine. *Reflecting Sunlight: Recommendations for Solar Geoengineering Research and Research Governance*. (The National Academies Press, 2021).

1329 220 Meng, J. *et al.* Improved Parameterization for the Size Distribution of Emitted Dust
1330 Aerosols Reduces Model Underestimation of Super Coarse Dust. *Geophysical Research Letters* **49**, doi:10.1029/2021gl097287 (2022).

1331 221 Slingo, J. *et al.* Ambitious partnership needed for reliable climate prediction. *Nature Climate Change* **12**, 499-503, doi:10.1038/s41558-022-01384-8 (2022).

1332 222 Myhre, G. *et al.* Radiative forcing of the direct aerosol effect from AeroCom Phase II
1333 simulations. *Atmospheric Chemistry and Physics* **13**, 1853-1877, doi:10.5194/acp-13-
1334 1853-2013 (2013).

1335 223 Okin, G. S. Where and How Often Does Rain Prevent Dust Emission? *Geophysical Research Letters* **49**, doi:10.1029/2021gl095501 (2022).

1336 224 Bergametti, G. *et al.* Rain, Wind, and Dust Connections in the Sahel. *Journal of Geophysical Research-Atmospheres* **127**, doi:10.1029/2021jd035802 (2022).

1337 225 Marsham, J. H., Knippertz, P., Dixon, N. S., Parker, D. J. & Lister, G. M. S. The
1338 importance of the representation of deep convection for modeled dust-generating winds
1339 over West Africa during summer. *Geophysical Research Letters* **38**,
1340 doi:10.1029/2011gl048368 (2011).

1341 226 Okin, G. S. A new model of wind erosion in the presence of vegetation. *Journal of Geophysical Research-Earth Surface* **113**, F02s10, doi:10.1029/2007jf000758 (2008).

1342 227 Chappell, A. & Webb, N. P. Using albedo to reform wind erosion modelling, mapping
1343 and monitoring. *Aeolian Research* **23**, 63-78, doi:10.1016/j.aeolia.2016.09.006 (2016).

1344 228 Huang, J. P. *et al.* Global semi-arid climate change over last 60 years. *Clim. Dyn.* **46**,
1345 1131-1150, doi:10.1007/s00382-015-2636-8 (2016).

1346 229 Prospero, J. M., Ginoux, P., Torres, O., Nicholson, S. E. & Gill, T. E. Environmental
1347 characterization of global sources of atmospheric soil dust identified with the Nimbus 7
1348 Total Ozone Mapping Spectrometer (TOMS) absorbing aerosol product. *Reviews of
1349 Geophysics* **40**, 1002, doi:10.1029/2000rg000095 (2002).

1350 230 Stanelle, T., Bey, I., Raddatz, T., Reick, C. & Tegen, I. Anthropogenically induced
1351 changes in twentieth century mineral dust burden and the associated impact on radiative
1352 forcing. *Journal of Geophysical Research-Atmospheres* **119**, 13526-13546,
1353 doi:10.1002/2014jd022062 (2014).

1354 231 Kohfeld, K. E. & Harrison, S. P. DIRTMAP: the geological record of dust. *Earth-Sci.
1355 Rev.* **54**, 81-114 (2001).

1356 232 Markle, B. R., Steig, E. J., Roe, G. H., Winckler, G. & McConnell, J. R. Concomitant
1357 variability in high-latitude aerosols, water isotopes and the hydrologic cycle. *Nature
1358 Geoscience* **11**, 853-+, doi:10.1038/s41561-018-0210-9 (2018).

1359 233
1360 234
1361 235
1362 236
1363 237
1364 238
1365 239

1366 233 Cowie, S. M., Knippertz, P. & Marsham, J. H. Are vegetation-related roughness changes
1367 the cause of the recent decrease in dust emission from the Sahel? *Geophysical Research*
1368 *Letters* **40**, 1868-1872, doi:10.1002/grl.50273 (2013).

1369 234 Smith, S. D. *et al.* Elevated CO₂ increases productivity and invasive species success in an
1370 arid ecosystem. *Nature* **408**, 79-82 (2000).

1371 235 Mahowald, N. M. Anthropocene changes in desert area: Sensitivity to climate model
1372 predictions. *Geophysical Research Letters* **34**, L18817, doi:10.1029/2007gl030472
1373 (2007).

1374 236 Goldewijk, K. K., Beusen, A., van Drecht, G. & de Vos, M. The HYDE 3.1 spatially
1375 explicit database of human-induced global land-use change over the past 12,000 years.
1376 *Global Ecology and Biogeography* **20**, 73-86, doi:10.1111/j.1466-8238.2010.00587.x
1377 (2011).

1378 237 Lee, J. A., Baddock, M. C., Mbuh, M. J. & Gill, T. E. Geomorphic and land cover
1379 characteristics of aeolian dust sources in West Texas and eastern New Mexico, USA.
1380 *Aeolian Research* **3**, 459-466, doi:10.1016/j.aeolia.2011.08.001 (2012).

1381 238 Neff, J. C. *et al.* Increasing eolian dust deposition in the western United States linked to
1382 human activity. *Nature Geoscience* **1**, 189-195, doi:10.1038/ngeo133 (2008).

1383 239 Webb, N. P. & Pierre, C. Quantifying Anthropogenic Dust Emissions. *Earth Future* **6**,
1384 286-295, doi:10.1002/2017ef000766 (2018).

1385 240 Niemeyer, T. C. *et al.* Optical depth, size distribution and flux of dust from Owens Lake,
1386 California. *Earth Surface Processes and Landforms* **24**, 463-479, doi:10.1002/(sici)1096-
1387 9837(199905)24:5<463::aid-esp2>3.0.co;2-r (1999).

1388 241 Xi, X. & Sokolik, I. N. Quantifying the anthropogenic dust emission from agricultural
1389 land use and desiccation of the Aral Sea in Central Asia. *Journal of Geophysical*
1390 *Research-Atmospheres* **121**, 12270-12281, doi:10.1002/2016jd025556 (2016).

1391 242 Indoitu, R. *et al.* Dust emission and environmental changes in the dried bottom of the
1392 Aral Sea. *Aeolian Research* **17**, 101-115, doi:10.1016/j.aeolia.2015.02.004 (2015).

1393 243 Tegen, I. & Fung, I. Contribution to the atmospheric mineral aerosol load from land-
1394 surface modification. *Journal of Geophysical Research-Atmospheres* **100**, 18707-18726,
1395 doi:10.1029/95jd02051 (1995).

1396 244 Sokolik, I. N. & Toon, O. B. Direct radiative forcing by anthropogenic airborne mineral
1397 aerosols. *Nature* **381**, 681-683 (1996).

1398 245 Mahowald, N. M., Rivera, G. D. R. & Luo, C. Comment on "Relative importance of
1399 climate and land use in determining present and future global soil dust emission" by I.
1400 Tegen *et al.* *Geophysical Research Letters* **31**, doi:10.1029/2004gl021272 (2004).

1401

1402 Acknowledgements

1403 J.F.K. is funded by the National Science Foundation (NSF) grants 1552519 and 1856389,
1404 A.T.E. is funded by NSF grant 1833173, N.M.M. is funded by Department of Energy (DOE)
1405 grant DE-SC0021302, and V.A.K. is supported by the European Union via its Horizon 2020
1406 project FORCeS (GA 81205). We thank James Hooper and Pierre Sabatier for providing dust
1407 deposition data.

1408 Competing interests

1409 The authors declare no competing interests.

1410 **Author contributions**

1411 J.F.K. led the review, performed the dust reconstruction, wrote the Supplementary material, prepared the
1412 figures, and compiled the paper. T.S. and A.A.A. contributed the section on clouds and figures 2c-f.
1413 V.A.K. contributed the section on atmospheric chemistry and figure 2b. N.M.M. contributed the section
1414 on biogeochemistry and a draft of figure 2h. C.H. contributed the section on the cryosphere and figure 2g.
1415 A.T.E. contributed the section on future dust changes. D.M.L. contributed to the CMIP6 results in figure
1416 5. All authors contributed to the manuscript preparation, discussion and writing.

1417 **Supplementary information**

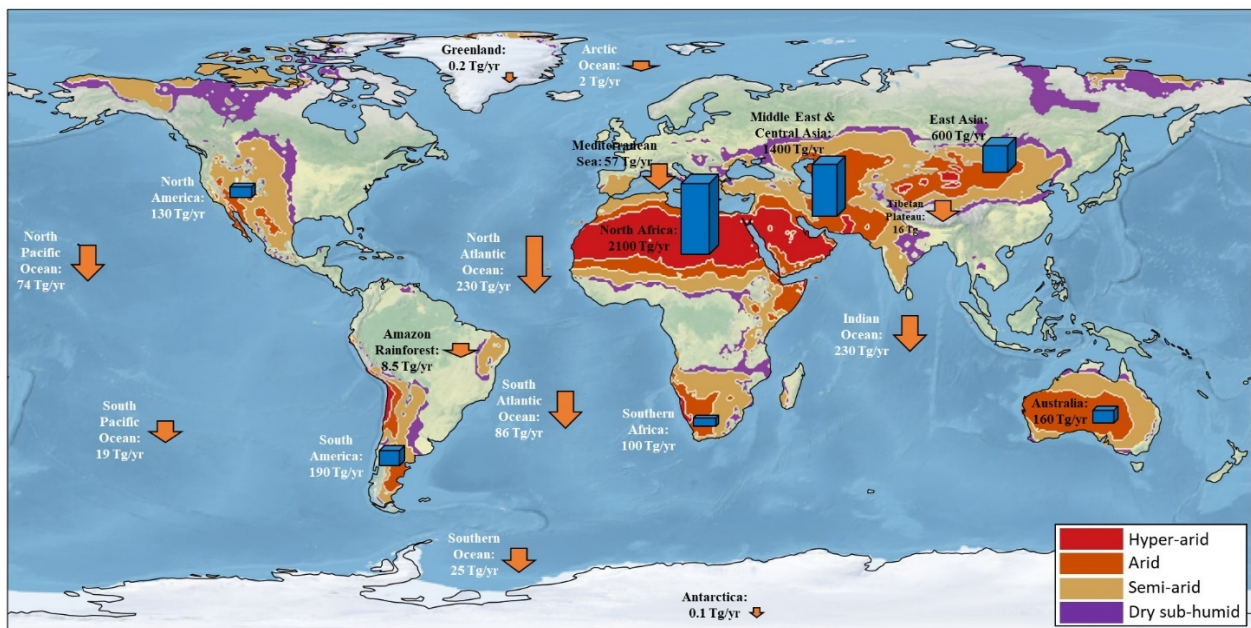
1418 Supplementary information is available for this paper at <https://doi.org/10.1038/s415XX-XXX-XXXX-X>
1419

1420 **Data availability**

1421 The dust reconstruction data shown in Figure 4 are available at [link to be added upon article acceptance].

1422 **Figure legends**

1423

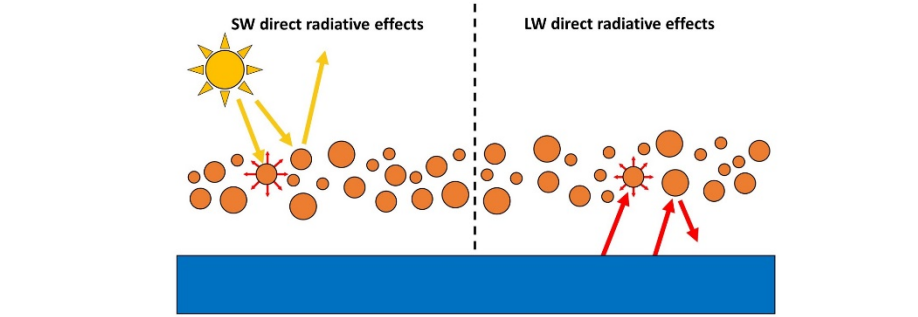


1424

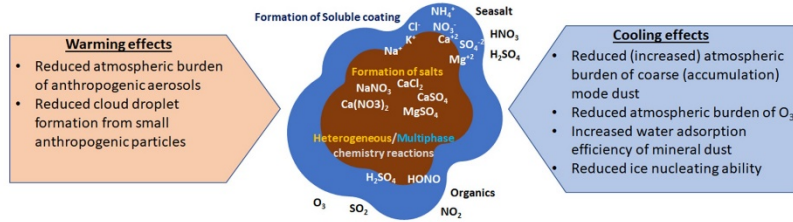
1425 **Figure 1. Main sources and sinks of dust in the global dust cycle.** Emission fluxes (blue bars) from the
1426 world's main dust source regions and deposition fluxes (orange arrows) to regions where dust can impact
1427 surface albedo or biogeochemistry. Fluxes are for dust with geometric (volume-equivalent) diameter up to
1428 20 μm and are based on constraints for 2004-2008⁴⁴; emissions from high latitude regions are not
1429 included. Shading represents dryland classification based on the aridity index: hyper-arid regions ($\text{AI} <$
1430 0.05; red shading), arid regions ($0.05 < \text{AI} < 0.20$; orange shading), semi-arid regions ($0.20 < \text{AI} < 0.50$;
1431 light brown shading), and dry sub-humid regions ($0.50 < \text{AI} < 0.65$; green shading)²²⁸. Most dust is
1432 emitted from drylands in North Africa and Asia, which are collectively known as the "dust belt"²²⁹.

1433

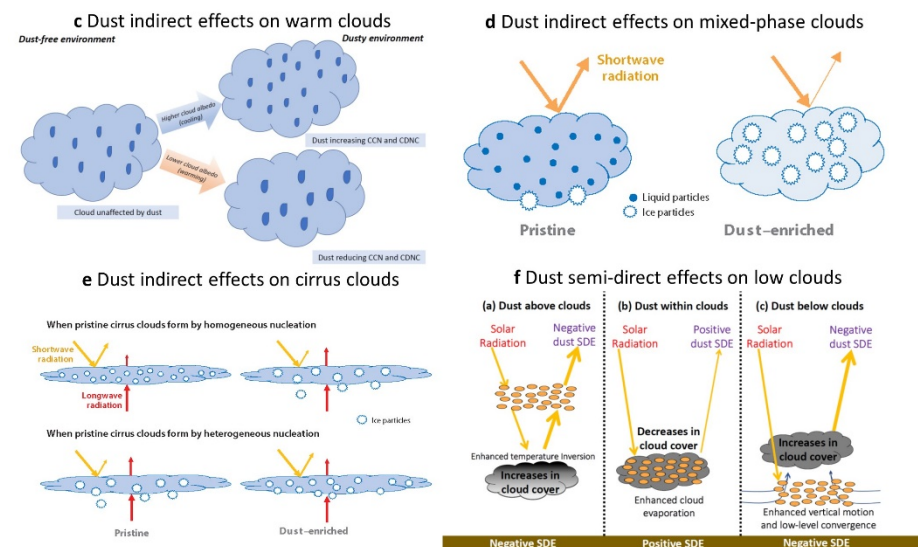
a Dust interactions with radiation



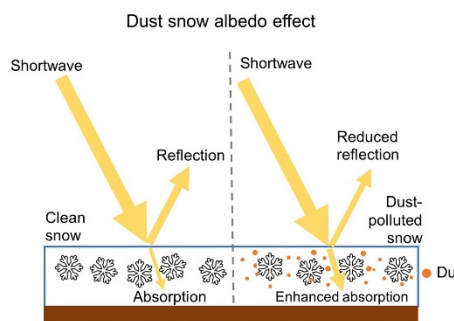
b Dust interactions with atmospheric chemistry



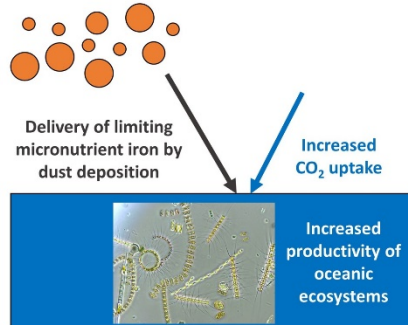
Dust interactions with clouds



g Dust interactions with the cryosphere



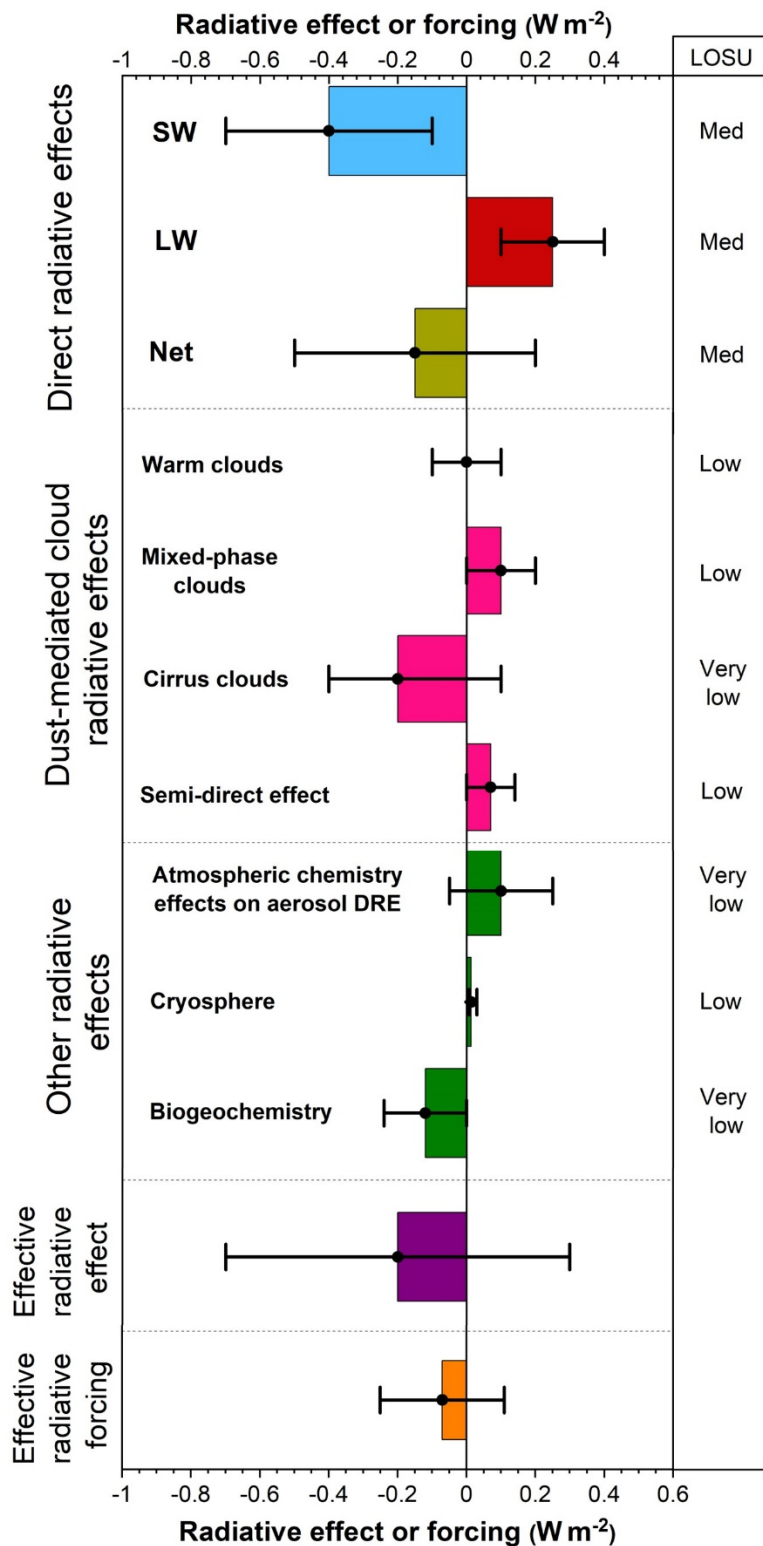
h Dust interactions with biogeochemistry



1435 **Figure 2. Mechanisms through which dust impacts climate.** **a** | dust direct interactions with shortwave
1436 (SW) and longwave (LW) radiation. **b** | dust interactions with atmospheric chemistry and the induced
1437 perturbations to the radiative fluxes at the top-of-atmosphere exerting a warming (left) or cooling (right)
1438 effect on global climate. The brown core represents the freshly emitted insoluble dust particle and the
1439 surrounding blue area represents the acquired soluble coating through interactions with atmospheric
1440 chemistry. **c** | dust indirect effects on warm clouds occur by dust increasing cloud albedo through adding
1441 to CCN and increasing CDNC (upper branch) and by dust decreasing cloud albedo by reducing non-dust
1442 CCN through enhanced particle coagulation and adsorption of precursor gases and by dust giant CCN
1443 reducing in-cloud supersaturation (lower branch). **d** | dust indirect effects on mixed-phase clouds (MPCs),
1444 illustrated by MPC formation in pristine (left) and dust-enriched (right) environments. **e** | dust indirect
1445 effects on cirrus clouds, separated by the dominant ice crystal formation mechanism in the absence of
1446 dust. **f** | dust semi-direct effects on low clouds due to local heating generated by dust absorption,
1447 separated by location of dust relative to clouds. **g** | radiative effects of dust deposited on snow and ice,
1448 illustrated by snow reflectivity without (left) and with (right) dust deposited onto the snowpack. **h** | effect
1449 of dust on CO_2 concentrations due to interactions with ocean biogeochemistry. Yellow arrows represent
1450 SW radiation and red arrows represent LW radiation.

1451

1452



1453
1454
1455
1456
1457

Figure 3. The global mean effective radiative effect and radiative forcing of dust at the top-of-atmosphere. Perturbations to Earth's radiation budget by dust through direct radiative effects, dust-mediated cloud radiative effects, and various other radiative effects. The sum of all radiative effects equals the dust effective radiative effect R (Eq. 2) and the portion of that dust effective radiative effect

1458 that is due to the increase in dust since pre-industrial times is the effective radiative forcing $\Delta F_{p \rightarrow m}$ (Eq.
1459 4). Error bars denote the 90% confidence range. The column on the right denotes the level of scientific
1460 understanding (LOSU), or confidence in the assessment of each radiative effect, following past practice²⁷.
1461 The global mean dust effective radiative effect and radiative forcing of dust are uncertain in sign and
1462 magnitude, but are more likely to cool than to warm the climate.

1463

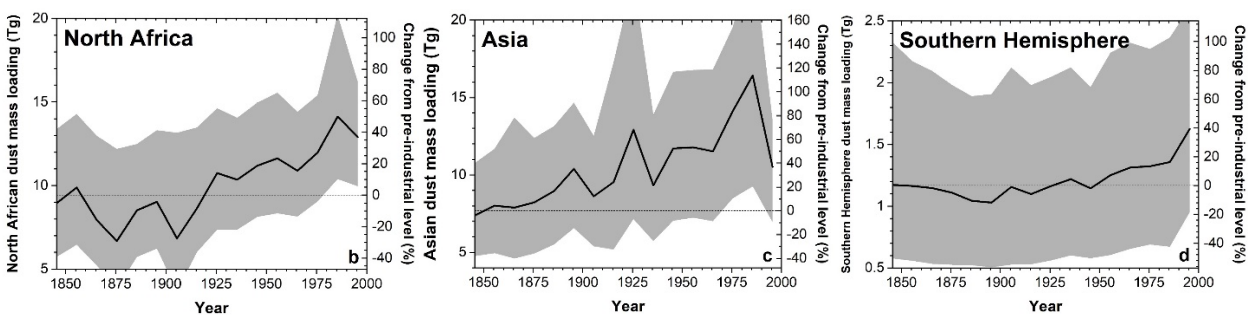
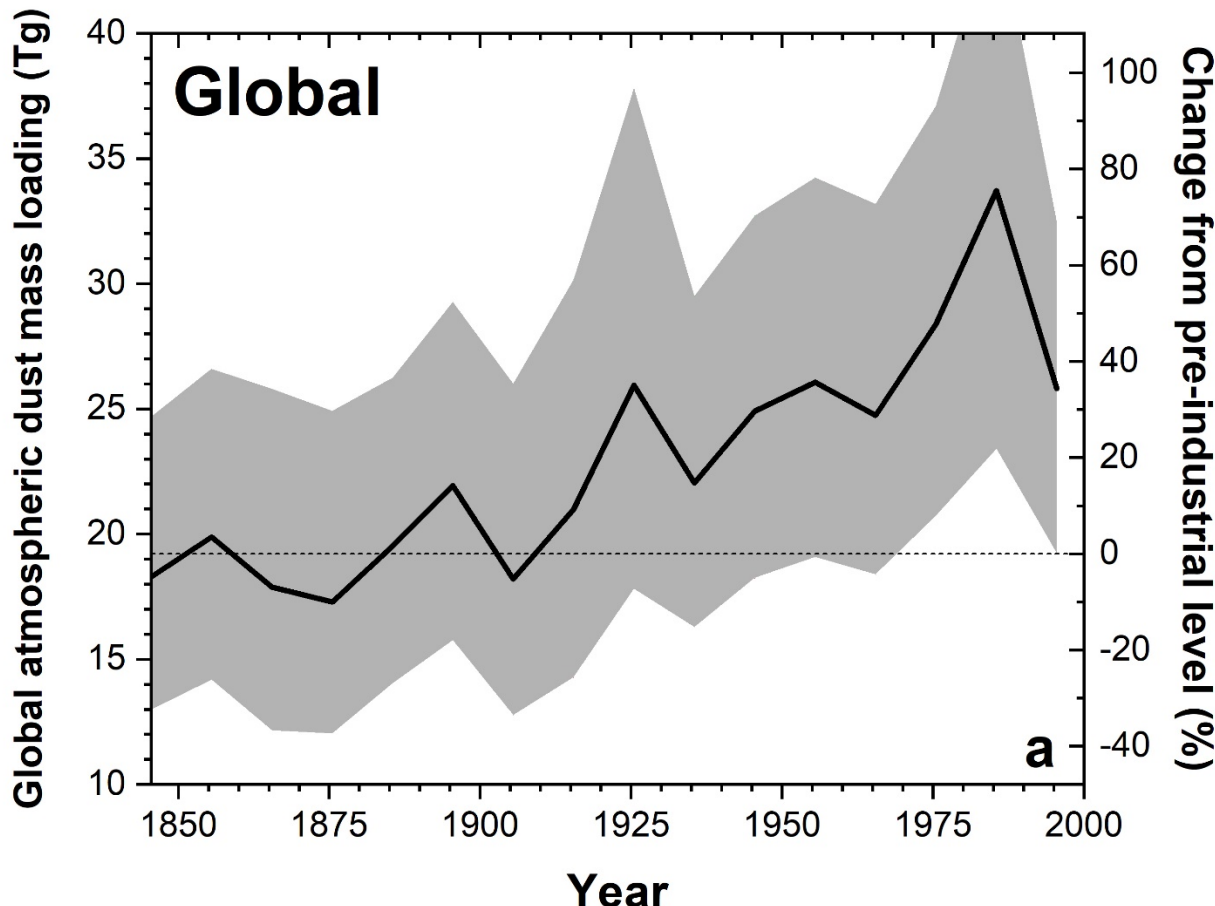
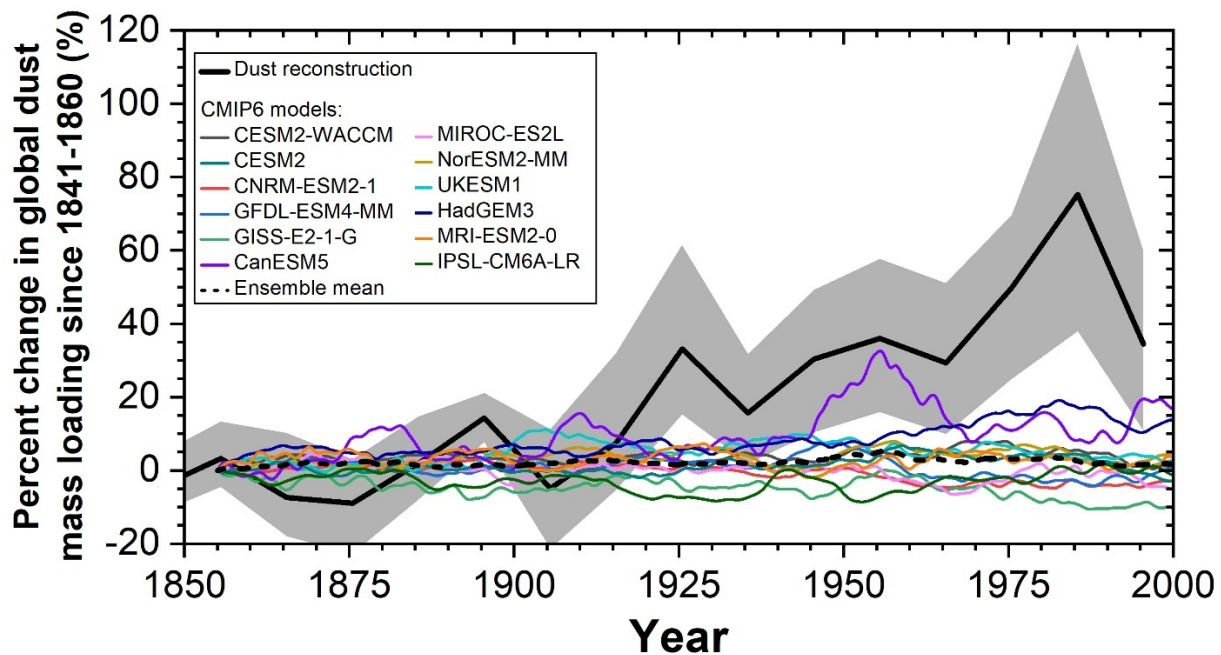


Figure 4. Atmospheric dust mass loading changes since pre-industrial times. a| Reconstructed globally integrated dust mass loading. **b|** as in a, but for loading contributed by dust from North Africa. **c|** as in a, but for loading contributed by dust from Asia. **d|** as in a, but for loading contributed by dust from the Southern Hemisphere. The solid line denotes the median dust loading estimate, the shading the 90% confidence range, and the dotted line the average pre-industrial (1841–1860) dust loading. Dust loadings were obtained by combining 22 records of dust deposition with constraints on the spatially resolved dust deposition fluxes produced by the world's main dust source regions^{8,44}; see Supplement for details. Dust has increased in all three regions, translating to a $56 \pm 29\%$ rise in global dust mass loading in modern times (1981–2000) compared to pre-industrial.

1466

1467



1469
1470 **Figure 5. Climate model representations of historical changes in dust loading.** Changes
1471 in global dust loading relative to the period 1841-1860 obtained from the dust reconstruction
1472 (solid black line) and simulated by 12 CMIP6 climate models with prognostic dust aerosol
1473 cycles²¹⁴ (thin colored lines). CMIP6 data are 10-year running means from historical runs¹⁸⁶.
1474 Grey shading denotes the 90% confidence interval for the dust reconstruction. All models
1475 and the ensemble mean (dashed black line) fail to reproduce the large historical increase in
1476 dust loading.

Box 1. Drivers of the historical increase in dust loading. The large historical increase in dust observed in deposition records and the reconstruction of dust mass loading (Fig. 4) can be either due to human land use changes or due to natural and anthropogenic changes in climate²³⁰.

The observational record shows that dust is highly sensitive to climate. Indeed, dust records in some regions show a variation of a factor of ~2-4 due to climate variability over the 20th century^{178,180,183} and dust has increased by a factor of ~2-4 in transitions between interglacial and glacial periods^{231,232}. As such, changes in aridity, vegetation cover, and wind speed due to natural climate variability could have driven (part of) the long-term increase in dust loading, as has been suggested for North Africa^{178,180,233}. In addition, anthropogenic changes to climate and atmospheric composition could also have affected dust loading, both by increasing aridity and by higher CO₂ concentrations fertilizing plants at desert margins²³⁴, with the net effect on desert extent and dust emissions still unclear²³⁵.

Human land use changes could also have increased dust emissions. The Industrial Revolution and the rise of industrialized agriculture have resulted in a dramatic increase in the area of land used by humans: the fraction of the ice-free land area used for agriculture has quadrupled from ~9% in 1850 to ~35% in 2000²³⁶. This large-scale conversion of wildlands to agricultural land has included many semi-arid and arid regions (Fig. 1), for which human land use changes can result in dramatic increases in dust emission²³⁷⁻²³⁹. Additionally, anthropogenic changes in water management that result in the drying of inland bodies of water might also have substantially increased dust emissions, such as has occurred for Owen's Lake in California in the early 20th century²⁴⁰ and more recently for the Aral Sea in Central Asia^{241,242}.

Modelling has been unable to determine whether the historical increase in dust, which models have been unable to reproduce²² (Fig. 5), has been primarily driven by climate or land use changes. Indeed, past research has diverged on the fraction of the global dust burden in the current climate emitted from anthropogenically disturbed sources, with results ranging from as little as 0% to as much as 50%^{199,207,230,243-245}. Similarly, modelling results on effects of changes in climate and CO₂ concentrations on dust loading also differ, with results varying between a decrease of -20% and an increase of +60% in dust loading^{199,230,235}.

Although large uncertainties thus remain in how climate and land use changes have contributed to the historical increase in dust loading (Fig. 4), two observational findings suggest that anthropogenic land use change has been a key driver of the long-term increase in dust loading (Fig. 4). First, the timing of increases in dust deposition in various deposition records appears to coincide with the rise of industrialized agriculture in source regions²³. And second, satellite observations suggest that ~25% of modern dust emissions originate from regions heavily impacted by human land use¹⁹¹. This finding implies that human land use changes have increased dust mass loading by ~33% since pre-industrial times, which accounts for the majority of the $56 \pm 29\%$ increase in dust mass loading since pre-industrial times (Fig. 4). Moreover, satellite observations indicate that the fraction of dust emitted from anthropogenically disturbed surfaces is substantially higher for Asian than for North African source regions, which is qualitatively consistent with the finding of a larger historical increase of Asian than of North African dust (Figs. 4b-d). Nonetheless, substantial additional work is

needed to determine the exact causes of the historical increase in dust for each of the world's main dust source regions.